Iteratively-improved Robin boundary conditions for the finite element solution of scattering problems in unbounded domains

S. Alfonzetti, G. Borzì, N. Salerno

Dipartimento Elettrico, Elettronico e Sistemistico - Universita' di Catania

Viale A. Doria, 6 - 95125 Catania - Italy

Tel.: +39 95 339535, Fax: +39 95 330793

E-mail: alfo@dees.unict.it

Keywords: Finite element method, scattering problems, open boundaries

Abstract

An iterative procedure is described for the finite-element solution of scalar scattering problems in unbounded domains. The scattering objects may have multiple connectivity, may be of different materials or with different boundary conditions. A fictitious boundary enclosing all the objects involved is introduced. An appropriate Robin (mixed) condition is initially guessed on this boundary and is iteratively improved making use of the Green formula. It will be seen that the best choice for the Robin boundary condition is an absorbing-like one. A theorem about the theoretical convergence of the procedure is demonstrated. An analytical study of the special case of a circular cylindrical scatterer is made. Comparisons are made with other methods. Some numerical examples are provided in order to illustrate and validate the procedure and to show its applicability whatever the frequency of the incident wave. Although particular emphasis is laid in the paper on electromagnetic problems, the procedure is fully applicable to other kinds of physical phenomena such as acoustic ones.

1. INTRODUCTION

As is well known scattering problems in open boundary domains are somewhat different from static or quasistatic ones because, to ensure the uniqueness of the solution, the Sommerfeld radiation condition must be imposed. Moreover the solution does not monotonically decrease to zero at infinity as in static problems, but oscillates while decaying.

For these reasons, in the context of the Finite Element Method (FEM)[1,2] a variety of techniques have been expressly devised for the solution of scattering problems in open boundaries.[3,4] These methods fall into two classes: exact methods which provide accurate results but generally lead to dense matrices, and approximate methods which provide less accurate results generating sparse matrices.

Exact methods include the Method of Moments (MoM), the various formulations of the hybrid FEM/BEM (Boundary Element Method[5]) and the infinite element method. By the MoM method the scalar Helmholtz equation is transformed into an integral equation[6] involving Green's function over the boundary of the domain where the differential equation has to be solved.[7,8] This method is very effective since it allows the problem dimensionality to be decreased by one, but produces fully populated system matrices. The major deficiencies of this method lie in possible internal resonances, especially at high frequencies, and on the restricted applicability to perfectly conducting objects. The FEM/BEM does not suffer from this last drawback. By this method a closed artificial surface separates an interior region, where an FEM discretization is set up, from an unbounded homogeneous exterior region. The exterior region is taken into account by means of an integral equation involving Green's function.[9,10] With this method one obtains an exact solution for the field, but the system matrix does not exhibit the advantageous properties of a standard FEM matrix; moreover for

the Helmholtz equation nearly singular matrices can be produced. In the infinite element method the unbounded domain is subdivided into a bounded circular region, which is discretized by means of finite elements, and an unbounded region, which is discretized by means of special unbounded elements, called infinite elements, whose shape functions resemble the asymptotic behaviour of the solution at infinity.[11,12] Due to these complicated shape functions this technique is difficult to implement. Moreover the use of a circle as truncation boundary may result in an excessively onerous free-space discretization.

The so-called Absorbing Boundary Condition (ABC) methods[13-15] are approximate methods in which the domain of interest is truncated to a region near the scatterer. A homogeneous local link between the field and its normal and/or tangential derivatives on the truncation boundary is imposed in such a way as to absorb the outgoing wave, avoiding the unreal presence of waves reflected from the boundary; the locality generates a sparse matrix. The use of derivatives of orders greater than the second is very rare, due to the inaccuracy with which they can be evaluated with an FEM approximation. ABC methods generally introduce errors in the solution, because the exact absorbing boundary condition on the border is not known *a priori*. The adaptive ABC technique proposed in [16] tries to overcome the last drawback by an iterative refining of a homogeneous absorbing boundary condition; this method, however, is non linear and may produce some numerical problems.[16] Another approximate method is the recent Measured Equation of Invariance (MEI) method,[17] in which the absorption of the outgoing wave is accomplished by modifying the equations relative to a suitable subset of nodes; the modification is determined by the shape of the scatterer and preserves the sparsity of the matrix. In certain cases the MEI method gives accurate results with low computational cost, but it may yield inaccurate solutions for problems involving dielectrics or concave boundaries.[16]

Recently the authors devised an iterative procedure to deal with unbounded electrostatic and skin-effect problems[18-20] which is very accurate and easy to implement in a pre-existing code for bounded problems. This procedure is based on an iterative improvement of a Dirichlet boundary condition on a fictitious boundary enclosing all the conductors of the problem.

In this paper a similar approach is proposed for the solution of scalar scattering problems, such as 2-D electromagnetic and 3-D acoustic ones. The main difference lies in the choice of a more general Robin (mixed) condition on the fictitious boundary which makes the procedure convergent whatever the initial guess for the Robin condition. The major advantages of this method are the complete absence of interior resonances whatever the frequency and its simplicity of implementation starting from a finite element code for bounded problems. In this paper the method is described in detail and validated by several numerical examples.

The structure of the paper is as follows: in Sect. 2 the iterative procedure is described for 2-D electromagnetic scattering; in Sect. 3 its convergence is studied both in numerical and analytical contexts; in Sect. 4 an analytical example is given regarding a circular cylinder; in Sect. 5 the extension to 3-D problems is discussed; in Sect. 6 comparisons are made with other methods whereas in Sect. 7 some numerical examples are given. The authors' conclusions follow in Sect. 8. Finally some implementation remarks are reported in Appendix A and a theoretical study of the procedure convergence is made in Appendix B.

2. THE ROBIN ITERATION PROCEDURE

Consider a system of N_S objects, made of conducting and/or dielectric materials, infinitely extended in the z-direction, surrounded by free space. The system is radiated by a given time-harmonic electromagnetic wave ###$_{inc}$, E- or H-polarized along the z-axis. So a scattered field ###$_s$ is excited extending to infinity. An unbounded problem is set up in terms of the total field ###, which outside the scatterers is given by ###$_{inc}$+###$_s$ and which everywhere satisfies the two-dimensional scalar Helmholtz equation

$$\nabla \cdot \frac{1}{\alpha} \nabla \phi + k_0^2 \eta \phi = 0 \tag{1}$$

In (1) ### is the electrical field E_z, ### is the relative magnetic permeability ###$_r$ and ### is the relative electrical permittivity ###$_r$ for the E-polarised case, whereas for the H-polarised one ### is the magnetic field H_z, ### is ###$_r$ and ### is ###$_r$; in both cases k_0 is the free-space wavenumber $k_0^2 = \omega^2 \varepsilon_0 \mu_0$, where ω is the wave angular frequency and μ_0 and ε_0 are the free-space magnetic permeability and electrical permittivity, respectively. Homogeneous Dirichlet and Neumann conditions hold on the perfect conductor surfaces, Γ_C, if any, for the E- and H-polarised cases, respectively. Moreover the scattered field ###$_s$ must satisfy the Sommerfeld radiation condition at infinity:

$$\lim_{r \to \infty} \sqrt{r} \left(\frac{\partial \phi_s}{\partial r} + j k_0 \phi_s \right) = 0 \tag{2}$$

where r is the distance of a point from the origin.

In order to compute the field in the proximity of (and inside) the scattering objects, they are enclosed in a fictitious boundary ###$_F$, where a Robin (mixed) boundary condition, expressed through the operator B, is initially imposed:

$$B\phi(\mathbf{r}) = \frac{\partial \phi(\mathbf{r})}{\partial n} + \kappa(\mathbf{r})\phi(\mathbf{r}) = \psi(\mathbf{r}) \qquad \mathbf{r} \in \Gamma_F \tag{3}$$

where κ and ψ are functions of point **r** on the fictitious boundary and where the normal derivative is calculated in the outward direction. Note that function κ is user-selected and does not change during the iterative procedure (a good choice is $\kappa = jk_0$, constant on ###$_F$), while ψ is first guessed and then iteratively improved, as explained later on.

By discretizing the bounded domain D, delimited by ###$_F$ and ###$_C$, by means of Lagrangian finite elements and applying the Galerkin method, the following set of algebraic equations is obtained:

$$\mathbf{A\Phi} = \mathbf{C\Psi} \tag{4}$$

where **A** is a square matrix depending on the geometry, dielectric materials and on the function κ, ### is the vector of the unknown nodal field values including that on the nodes of ###$_F$, **Ψ** is the vector of the nodal values of the right hand-side of the Robin condition on ###$_F$ and **C** is a rectangular matrix that links the values of the Robin condition on the fictitious boundary with the known terms of the system.

Consider now another closed curve, ###$_M$, lying between the scattering objects and the fictitious boundary (see Fig. 1). At minimum this curve can be selected as coinciding with the

surface $\#\#\#_S$ of the scatterring objects themselves. The total field outside $\#\#\#_M$ can be expressed as:[21]

$$\phi(\mathbf{r}) = \phi_{inc}(\mathbf{r}) - \int_{\Gamma_M} \left\{ G(\mathbf{r},\mathbf{r}') \frac{\partial \phi(\mathbf{r}')}{\partial n'} - \phi(\mathbf{r}') \frac{\partial G(\mathbf{r},\mathbf{r}')}{\partial n'} \right\} ds' \tag{5}$$

where n' is the outward normal to $\#\#\#_M$ (toward $\#\#\#_F$), and $G(\mathbf{r},\mathbf{r}')$ is the free-space Green's function, which in the two-dimensional case is given by: [21]

$$G(\mathbf{r},\mathbf{r}') = -\tfrac{1}{4} j H_0^{(2)}\left(k_0 |\mathbf{r} - \mathbf{r}'|\right) \tag{6}$$

where $H_0^{(2)}$ is the zero-order Hankel function of the second kind. By virtue of (5) function ψ can be expressed as:

$$\psi(\mathbf{r}) = B\,\phi(\mathbf{r}) = B\,\phi_{inc}(\mathbf{r}) - \int_{\Gamma_M} \left\{ \frac{\partial \phi(\mathbf{r}')}{\partial n'} B\,G(\mathbf{r},\mathbf{r}') - \phi(\mathbf{r}') \frac{\partial B\,G(\mathbf{r},\mathbf{r}')}{\partial n'} \right\} ds' \qquad \mathbf{r} \in \Gamma_F \tag{7}$$

Conveniently selecting the curve Γ_M as constituted of element sides only and employing the finite element field approximation, this relation is rewritten as (see Appendix A for computational details):

$$\boldsymbol{\Psi} = \boldsymbol{\Psi}_{inc} + \mathbf{M}\boldsymbol{\Phi} \tag{8}$$

where $\boldsymbol{\Psi}_{inc}$ is the vector of the values of the operator B applied to the incident field on the nodes of the fictitious boundary and **M** is a rectangular matrix in which null columns appear for the nodes not belonging to the elements external to $\#\#\#_M$ and having a side lying on it.

Equations (4) and (8) together form the global algebraic system:

$$\begin{bmatrix} \mathbf{A} & -\mathbf{C} \\ -\mathbf{M} & \mathbf{I} \end{bmatrix} \begin{bmatrix} \boldsymbol{\Phi} \\ \boldsymbol{\Psi} \end{bmatrix} = \begin{bmatrix} 0 \\ \boldsymbol{\Psi}_{inc} \end{bmatrix} \tag{9}$$

which can be efficiently solved with a block Gauss-Seidel iteration scheme:[22]

$$\begin{aligned} \mathbf{A}\boldsymbol{\Phi}^{(m)} &= \mathbf{C}\boldsymbol{\Psi}^{(m)} \\ \boldsymbol{\Psi}^{(m+1)} &= \boldsymbol{\Psi}_{inc} + \mathbf{M}\boldsymbol{\Phi}^{(m)} \end{aligned} \tag{10}$$

This scheme is as follows:

i) having selected a suitable Robin operator, at the beginning the vector $\boldsymbol{\Psi}$ is guessed arbitrarily;

ii) equation (4) is solved for the vector $\boldsymbol{\Phi}$**;**

iii) another guess for the Robin condition on $\#\#\#_F$ is obtained by means of (8);

iv) if the solution is accurate enough the procedure stops; otherwise it goes back to ii).

This procedure can be made computationally efficient if the following points are fully exploited in implementation.

a) Matrices **A**, **M** and **C** do not change during the iterations, so that they are computed only once, at the beginning of the procedure.

b) Since a standard FE problem is set up at each step, equation (4) may be solved efficiently by means of standard solvers, which exploit the matrix **A** sparsity and symmetry; if an iterative solver is used the solution at step m is a good initial guess for the solver at step m+1 and the preconditioner,[23] if any, is calculated only once; if a direct solver is used the decomposition of **A** is carried out only once.

c) By suitably placing the fictitious boundary around the scattering objects, small extensions of the domain D can be obtained; as will be shown in the following, the distance for which convergence takes place in a few iterations is very short with respect to that necessary to find an acceptable solution by other methods, such as ABC ones. Moreover, if the fictitious boundary is constituted by several closed curves, each one enclosing a scattering object, the domain is subdivided into N_S disjoint pieces and the global FEM system (4) is partitionable into N_S independent subsystems, with a consequent decreasing of the overall computing time.

d) Since convergence of the Robin condition on the boundary Γ_F assures convergence of the field solution in the domain D, the end-iteration test is conveniently restricted to the fictitious boundary (see Appendix A for details).

e) If the selected Robin boundary operator resembles an ABC one, the optimal initial guess for $\boldsymbol{\Psi}^{(0)}$ is $\boldsymbol{\Psi}_{inc}$ so that the number of iterations are minimized.

These features make the Robin iteration procedure competitive with respect to other techniques as far as computing time and memory requirements are concerned. In addition the procedure is easy implementable in a pre-existing FEM code for bounded problems. Mainly only one routine has to be developed which calculates the matrix **M.** Note that no singularities arise in these calculations since the fictitious boundary Γ_F is placed at a given distance from Γ_M.

3. CONVERGENCE OF THE PROCEDURE

In order to investigate the convergence properties of the procedure, the true values (in the FE approximation) of the field $\mathbf{\Phi}_t$ and of the Robin condition $\mathbf{\Psi}_t$ are introduced. These values are those relative to the solution of the unbounded scattering problem. The initial guess $\mathbf{\Psi}^{(0)}$ is related to $\mathbf{\Psi}_t$ by means of the error vector $\mathbf{\Psi}_e^{(0)}$:

$$\mathbf{\Psi}^{(0)} = \mathbf{\Psi}_t + \mathbf{\Psi}_e^{(0)} \tag{10}$$

Of course this relation is only formal since both terms on the right side are unknown.

Solving equation (4) for the vector $\mathbf{\Phi}$, we obtain the field solution at the 0th step:

$$\mathbf{\Phi}^{(0)} = \mathbf{A}^{-1}\mathbf{C}\mathbf{\Psi}_t + \mathbf{A}^{-1}\mathbf{C}\mathbf{\Psi}_e^{(0)} \tag{11}$$

in which the first term gives, by definition, the true field solution:

$$\mathbf{\Phi}_t = \mathbf{A}^{-1}\mathbf{C}\mathbf{\Psi}_t \tag{12}$$

whereas the second one represents the field error:

$$\mathbf{\Phi}_e^{(0)} = \mathbf{A}^{-1}\mathbf{C}\mathbf{\Psi}_e^{(0)} \tag{13}$$

Starting from this solution, the new guess for the Robin condition on Γ_F is computed as:

$$\boldsymbol{\Psi}^{(1)} = \boldsymbol{\Psi}_{inc} + \mathbf{M}\boldsymbol{\Phi}_t + \mathbf{M}\boldsymbol{\Phi}_e^{(0)} \tag{14}$$

By virtue of (12), (13) and (14) and taking into account that:

$$\boldsymbol{\Psi}_t = \boldsymbol{\Psi}_{inc} + \mathbf{M}\boldsymbol{\Phi}_t \tag{15}$$

the error at the 1st step on the Robin condition is:

$$\boldsymbol{\Psi}_e^{(1)} = \mathbf{P}\,\boldsymbol{\Psi}_e^{(0)} \tag{16}$$

where $\mathbf{P}$ is a square matrix of order N_F (number of nodes on Γ_F) given by:

$$\mathbf{P} = \mathbf{M}\mathbf{A}^{-1}\mathbf{C} \tag{17}$$

With the new boundary condition (14), another field solution is obtained, whose error is:

$$\boldsymbol{\Phi}_e^{(1)} = \mathbf{A}^{-1}\mathbf{C}\mathbf{P}\,\boldsymbol{\Psi}_e^{(0)} \tag{18}$$

By further continuing the procedure, we can generalize (16) and (18) for the generic m-th step:

$$\boldsymbol{\Psi}_e^{(m)} = \mathbf{P}^m\,\boldsymbol{\Psi}_e^{(0)} \tag{19}$$

$$\mathbf{\Phi}_e^{(m)} = \mathbf{A}^{-1}\mathbf{C}\mathbf{P}^m \mathbf{\Psi}_e^{(0)} \tag{20}$$

Hence the procedure converges to the true solution for every initial error $\mathbf{\Psi}_e^{(0)}$ if and only if the spectral radius ρ of matrix **P** is lower than 1. Otherwise divergence may occur.

By the definition (17) of matrix **P** it emerges that the spectral radius ρ depends in a very complicated manner on the distance of $\#\#\#_F$ from the scatterers, on the whole FE discretization, on the function κ and on the frequency. In addition it is not feasible to check condition $\rho<1$ at the beginning of the iterative procedure, since matrix **P** is not available. On the other hand the derivation of criteria implying $\rho<1$ is essential for a practical application of the procedure. As will be seen in the following, these criteria are concerned with the placement of the fictitious boundary around the scattering objects. In order to obtain more insights on this item a theoretical study is made in Appendix B, without referring to the finite element discretization. By performing the steps foreseen by the procedure in a theoretical way (by means of equations (1) and (7)) the sequence of Robin condition errors $\psi_e^{(0)}(\mathbf{r}), \psi_e^{(1)}(\mathbf{r}),\ldots, \psi_e^{(m)}(\mathbf{r}), \mathbf{r} \in \Gamma_F$, is obtained. By defining the quadratic norm:

$$\|\psi\|_F = \left(\int_{\Gamma_F} |\psi|^2 \, d\Gamma \right)^{1/2} \tag{21}$$

the following theorem holds for this sequence:

THEOREM For a system of perfectly-conducting objects enclosed by a circular fictitious boundary of radius R_F on which a Robin condition (with $\kappa=jk_0$) is imposed, the sequence of the Robin condition errors is such that:

$$\left\|\psi_e^{(m)}\right\|_F \le \bar{\rho}^m \left\|\psi_e^{(0)}\right\|_F \qquad \forall\ m = 1,2,\ldots\infty \tag{22}$$

where $\bar{\rho}$ is a suitable real constant, depending on geometry only, which vanishes asymptotically as $O(R_F^{-1})$ as $R_F \to \infty$.

The proof of this theorem (see Appendix B) has been given thanks to the fact that the Robin operator employed resembles an ABC one. A simple absorbing operator has been used, but it can be seen that more sophisticated operators, such as those derived in [13,14] may also be used.

From the theorem it is clear that by opportunely distancing the circular fictitious boundary from the conductors, it is possible to obtain values of $\bar{\rho}$ less than 1 (contraction coefficient), so that the sequence of the error norms tends to zero and the procedure converges to the exact solution. Unfortunately the theorem does not give an exact rule for the choice of the radius R_F of the fictitious boundary, but it is not only an existence theorem, because it shows the asymptotic behaviour of the contraction coefficient.

In order to obtain practical criteria for the placement of the fictitious boundary, in the next section they are derived for the classical problem of a single circular cylinder. By means of a set of more complex examples, these criteria will be experimentally tested to prove their general validity for systems with arbitrarily-shaped scatterers, possibly made of penetrable materials.

4. AN ANALYTICAL EXAMPLE: THE CIRCULAR CYLINDER

This section is devoted to the analytical study of a simple system constituted by an infinite, perfectly-conducting cylinder with circular cross section of radius R embedded in free space. A cylindrical coordinate frame r, φ, z is set having the z-axis coincident with the cylinder axis.

The cylinder is irradiated by an incident electromagnetic wave, E- or H-polarized along the z-axis. This wave can be decomposed into a series of cylindrical waves of the form:[21]

$$\phi_{inc} = \sum_{n=-\infty}^{n=+\infty} a_n J_n(k_0 r)\, e^{jn\varphi} \tag{23}$$

where J_n is the Bessel function of the first kind and order n, and a_n are complex coefficients depending on the incident wave (plane, cylindrical, etc.).

Since the response to an incident cylindrical wave of order n is an outgoing cylindrical wave of the same order, the solution of this scattering problem is given by:

$$\phi_s = \sum_{n=-\infty}^{n=+\infty} a_n b_n H_n^{(2)}(k_0 r)\, e^{jn\varphi} \tag{24}$$

where $H_n^{(2)}$ is the Hankel function of the second kind and order n and b_n are complex coefficients given by:[21]

$$b_n = -\frac{J_n(k_0 R)}{H_n^2(k_0 R)} \qquad (\text{E} - \text{polarized wave}) \tag{25}$$

$$b_n = -\left.\frac{dJ_n(k_0 r)/dr}{dH_n^2(k_0 r)/dr}\right|_{r=R} \qquad (\text{H} - \text{polarized wave}) \tag{26}$$

In order to study the behaviour of the iterative procedure in solving this scattering problem, a fictitious boundary ###$_F$ is selected as a circumference of radius R_F=R+d, (d>0), centered at the origin. A rather more general Robin boundary condition is initially imposed on the fictitious boundary and developed in the Fourier series of the φ co-ordinate:

$$B\phi = \beta\frac{\partial\phi}{\partial r} + \kappa\phi = \psi^{(0)} = \sum_{n=-\infty}^{n=+\infty}\mu_n^{(0)} e^{jn\varphi} \tag{27}$$

so that for β=0 and κ≠0 we have Dirichlet conditions, for β≠0 and κ=0 Neumann conditions and for β≠0 and κ≠0 Robin ones. On the conductor surface homogeneous Dirichlet or Neumann boudary conditions hold for E- or H-polarized waves, respectively.

With the above boundary conditions the solution of the Helmholtz equation in the bounded circular shell D, delimited by Γ_C and ###$_F$, is given by:

$$\phi^{(0)}(r,\varphi) = \sum_{n=-\infty}^{+\infty}\mu_n^{(0)}\,\tau_n(r)\; e^{jn\varphi} \tag{28}$$

where functions $\tau_n(r)$ are the solutions of the following one-dimensional boundary-value problems:

$$\frac{1}{\alpha}\frac{d^2\tau_n}{dr^2}+\frac{1}{\alpha\, r}\frac{d\tau_n}{dr}+\left(k_0^2\eta-\frac{n^2}{r^2}\right)\tau_n=0 \qquad \text{in } (R, R_F)$$

$$\left[\beta\frac{d\tau_n(r)}{dr}+\kappa\tau_n(r)\right]_{r=R_F}=1 \tag{29}$$

$$\tau_n(R)=0 \qquad (E-\text{polarized wave})$$

$$\left.\frac{d\tau_n(r)}{dr}\right|_{r=R}=0 \qquad (H-\text{polarized wave})$$

Starting from this solution a new guess $\psi^{(1)}$ for the Robin condition on the fictitious boundary is computed by means of (7) in which the intermediate curve $\#\#\#_M$ is conveniently selected as coinciding with the conductor surface $\#\#\#_C$ ($\equiv\#\#\#_S$) itself. In this computation one can see that the n-th term of the Fourier series of $\psi^{(0)}$ influences only the n-th term of $\psi^{(1)}$, namely

$$\mu_n^{(1)}=\gamma_n+\rho_n\,\mu_n^{(0)} \tag{30}$$

where:

$$\gamma_n=a_n\left[\beta\, dJ_n(k_0\, r)/dr+\kappa\, J_n(k_0 r)\right]_{r=R_F} \tag{31}$$

$$\rho_n=\left(1+\frac{1}{b_n}\left[\frac{\beta\, dJ_n(k_0\, r)/dr+\kappa\, J_n(k_0\, r)}{\beta dH_n^2(k_0 r)/dr+\kappa\, H_n^2(k_0\, r)}\right]_{r=R_F}\right)^{-1} \tag{32}$$

In order to perform a convergence analysis like that in Section 3, let us introduce the true Robin boundary condition ψ_t on Γ_F and develop it in Fourier series:

$$\psi_t = \sum_{n=-\infty}^{n=+\infty} \mu_{tn} e^{jn\varphi} \tag{33}$$

Function $\psi_t(\mathbf{r})$, $\mathbf{r} \in \Gamma_F$, must be such that, by setting $\psi^{(0)} = \psi_t$ in the application of the iterative procedure, at step 1 one obtains again $\psi^{(1)} = \psi_t$. Then for this case equation (30) is rewritten as:

$$\mu_{tn} = \gamma_n + \rho_n \mu_{tn} \tag{34}$$

Subtracting (34) from (30), we have

$$\mu_n^{(1)} - \mu_{tn} = \rho_n \left(\mu_n^{(0)} - \mu_{tn} \right) \tag{35}$$

The meaning of ρ_n is now clear: it is the contraction coefficient of the n-th Fourier coefficient of the Robin boundary condition error. Hence the procedure is convergent to the true solution whatever the initial error on the Robin condition on the fictitious boundary if and only if all the contraction coefficients ρ_n have modulus less than 1:

$$|\rho_n| < 1 \qquad \forall\, n \tag{36}$$

At this point some important remarks can be made regarding the reasons why the Dirichlet and Neumann versions of the procedure do not work very well. In fact assume that a

Dirichlet condition is imposed on the fictitious boundary instead of a Robin one; then by setting $\beta=0$ in (32) the n-th contraction coefficient changes into:

$$\rho_n = \left(1 + \frac{1}{b_n}\,\frac{J_n(k_0 R_F)}{H_n^{(2)}(k_0 R_F)}\right)^{-1} \tag{37}$$

This coefficient is equal to 1 for all the placements of the fictitious boundary such that $R_F = x_{nk}/k_0$ where x_{nk} is the k-th zero of the Bessel function $J_n(x)$. Since these zeroes form an unlimited countable set, the contraction coefficient ρ_n does not decrease to zero for increasing R_F, and, more than that, it is not bounded by a quantity less than 1 when R_F tends to infinity. The higher the frequency, the higher the number of harmonics involved in the procedure, so that it becomes more difficult to find a fictitious boundary such that the procedure does not diverge. For the case of a perfectly-conducting circular cylinder lighted up by an E-polarized wave direct numerical calculations show that the procedure exhibits an acceptable convergence only for $\lambda>R$, whereas for $\lambda<R/2$ it is divergent for any placement of the fictitious boundary.

The same drawbacks arise in the Neumann version of the procedure; setting $\kappa=0$, the n-th contraction coefficient becomes:

$$\rho_n = \left(1 + \frac{1}{b_n}\left[\frac{dJ_n(k_0 r)/dr}{dH_n^2(k_0 r)/dr}\right]_{r=R_F}\right)^{-1} \tag{38}$$

which is equal to 1 for $R_F = y_{nk}/k_0$, where y_{nk} is the k-th zero of the Bessel function derivative $dJ_n(y)/dy$.

Consider now the case in which a Robin boundary condition is imposed on Γ_F. Without loss of generality we can set $\beta=1$. The function $\kappa(\mathbf{r})$ is optimally selected in such a way as to minimize the contraction coefficients ρ_n. Making use of the asymptotic approximations of the Bessel and Hankel functions, one can see that the optimal choice of κ is

$$\kappa(R_F) = jk_0 + \xi(R_F) \tag{39}$$

where $\xi(R_F)$ is an arbitrary function which vanishes at least as $O\left(R_F^{-1}\right)$ with $R_F \to \infty$. In this way all the coefficients ρ_n vanish as $O\left(R_F^{-1}\right)$.

This choice, although obtained for great values of R_F, will be employed, with $\xi=0$, also for fictitious boundaries placed near the scattering object. Consequently:

$$\rho_n = \left(1 + \frac{1}{b_n} \left[\frac{dJ_n(k_0 r)/dr + j k_0 J_n(k_0 r)}{dH_n^2(k_0 r)/dr + j k_0 H_n^2(k_0 r)} \right]_{r=R_F} \right)^{-1} \tag{40}$$

In Fig. 2 the distance d_n such that $|\rho_n| =1$ is plotted for several values of n (ranging from 0 to 45), versus the cylinder radius R for the E-polarized case. For $d>d_n$ we have $|\rho_n| <1$, whereas for $d<d_n$ we have $|\rho_n| >1$. Both the distance d_n and the radius R are normalized by multiplication by the free space wavenumber k_0. The n-th curve attains its maximum for a normalized radius nearly equal to n+1 and this maximum value increases with the order. In Fig. 3 the same distance is plotted for the H-polarized case, with n ranging from 0 to 30. In this case the maximum is constant for the various harmonics. From these results it can be seen

that the procedure is unconditionally convergent to the true solution if the fictitious boundary is placed at a distance d greater than a minimum one $d_{min} = \max d_n$, approximately given by:

$$k_0 d_{min} = \begin{cases} 0.278\sqrt{k_0 R - 10.9} - 0.326 & \text{for } k_0 R \geq 12.3 \\ 0 & \text{otherwise} \end{cases} \quad (\text{E} - \text{polarized wave})$$
$$k_0 d_{min} = 0.078 \quad (\text{H} - \text{polarized wave}) \qquad (41)$$

According to these formulas the fictitious boundary can be placed very near to the surface of the scattering object, so that little space around it needs to be meshed in the numerical version of the procedure. Note that the distance d_{min} does not constitute the optimal choice for the placement of the fictitious boundary as far as computing time is concerned. In fact, in this case some contraction coefficients ρ_n have modulus a little less than 1, and consequently a great number of iterations are to be expected. So it is convenient to place the fictitious boundary at a greater distance (2-3 d_{min}) in such a way that all the contraction coefficients have modulus significantly less than 1. Although formulae (41) have been derived for scattering from a perfectly-conducting circular cylinder, they have been experimentally observed for other shapes of perfectly-conducting objects and fictitious boundaries, provided that R is interpreted as the mean radius of the scatterer.

Finally note that a similar study could also be made in the case of circular cylinders made of of a non perfectly-conducting material having constitutive parameters defined by two radial functions $\alpha(r)$ and $\eta(r)$. In this case equation (40) is still valid provided the values of b_n are different. Moreover one can still employ (41) with good approximation to distance the fictitious boundary from non circular scatterers made of penetrable materials.

5. ROBIN ITERATION PROCEDURE FOR 3-D PROBLEMS.

The Robin iteration procedure described in Sect. 2 has characteristics of N-dimensionality since 3-D and axisymmetric versions can be implemented from a suitable 2-D one with minor changes, as explained in the following. Of course the 3-D version does not apply to electromagnetic phenomena, since in this case both the equation and the Robin boundary condition change in a vectorial manner so that several parts of this paper should be substantially modified (see for example Appendix B). However there exist several kinds of 3-D physical phenomena, such as acoustic ones, which are governed by the scalar Helmholtz equation and to which the Robin iteration procedure is fully applicable.

In the 3-D version of the procedure the main changes are concerned with the Green's function to be used, which in this case is given by:

$$G(\mathbf{r},\mathbf{r}') = -\frac{e^{-jk_0|\mathbf{r}-\mathbf{r}'|}}{4\pi|\mathbf{r}-\mathbf{r}'|} \tag{42}$$

Of course both Γ_F and Γ_M are now closed surfaces. In particular the integration surface Γ_M is conveniently constituted by finite element sides, that is, triangles or quadrangles for tetrahedral or brick elements, respectively.

As regards implementation, all the formulae reported in Appendix A also hold in the 3-D case, so that one can develop a single computer code which works both in two and three dimensions, simply according to the value of a dimensional index.[24,25]

Moreover the theoretical study of Appendix B and, in particular, the theorem stated in Sect. 3, are also fully applicable to 3-D problems.

6. COMPARISONS WITH OTHER METHODS

In this Section the Robin iteration procedure is compared with other exact methods for the solution of scattering problems in open boundary domains. Comparisons with approximated methods will be made in the next Section by means of numerical examples.

A first comparison is made with the hybrid FEM/BEM method. It is well known that it is possible to have a non zero incident wave which is zero on the artificial boundary, so that by using Dirichlet boundary conditions on the artificial boundary the incident field is not properly represented in the formulation. Following[10] the known term vector of a FEM/BEM system depends linearly on the values of the incident field on the artificial boundary which encloses the scatterer, while the vector of unknowns represents the nodal values of the total field. If there exists a non zero incident wave which is zero on the artificial boundary, then the vector of known terms is zero while the vector of unknowns is not zero, that is to say the system matrix is singular. For general geometries the system matrix will not be singular, but it may be ill conditioned, especially at high frequencies. In fact it has been observed that iterative solvers fail to converge when the frequency is higher than a critical value which is of the order of the lowest resonant frequency of the discretized region.[26] The same problem arises in the the MoM method and is known as 'interior resonance.'[27]

These disadvantages do not appear in the Robin iteration procedure. In fact let ϕ be a solution of the Helmholtz equation in a homogeneous domain D on whose boundary a homogeneous Robin condition with $\kappa=jk_0$ is imposed (i.e. $\psi=0$). Since the quadratic norms of ϕ and $\partial\phi/\partial n$ on the boundary are bounded by $k_0^{-1}\|\psi\|_F$ and $2\|\psi\|_F$ (see Lemma 1 in Appendix B), respectively, both ϕ and $\partial\phi/\partial n$ vanish on the boundary so that ϕ vanishes inside D. Hence the known term of the global algebraic system (9) resulting from the application of the Robin

iteration procedure is zero if and only if the physical source is zero. In other words the Robin iteration procedure global system (9) is well conditioned whatever the frequency of the incident wave. A disadvantage of the proposed method with respect to FEM/BEM is the need to mesh an air gap around the scattering objects, which, however, can be selected very thin, as shown in Sect. 4, and allows singularities in the computation of the integral equation coefficients to be avoided.

A second comparison is made with the infinite element method. Although this is an exact method its implementation is not simple since the interpolating functions of exterior elements must follow the asymptotic behaviour of the solution $r^{-1/2}\exp(jk_0r)$, whose oscillatory term prevents the use of simple analytical or numerical integration techniques. Moreover the bounded region must be a circle or a sphere, so its discretization may be storage intensive and numerically inefficient, as for instance when the system is composed of several objects separated by distances much greater than their diameters. These drawbacks are absent in the Robin iteration procedure since the fictitious boundary can be selected as constituted of several parts, each one enclosing a single scattering object.

The last comparison is made with the adaptive ABC proposed in [16]. This technique is very effective and accurate and is similar to the one described in this paper. The main difference lies in the fact that the adaptive ABC assigns a fixed value of 0 to the right-hand side of the ABC (Robin) boundary condition for the scattered field on the artificial border, and updates the coefficient κ at each iteration by setting

$$\kappa^{(m+1)} = -\frac{1}{\phi_s^{(m)}}\frac{\partial \phi_s^{(m)}}{\partial n} \tag{43}$$

where $\phi_s^{(m)}$ is given by (5) without the first term referring to the incident field. This technique, however, has some disavantages. First the global system matrix changes at each step of the procedure. Secondly it may happen that $\phi_s^{(m)} \approx 0$ on some points of the artificial boundary, so that the procedure stops by an overflow error or becomes oscillatory. Thirdly the technique is non linear, so its global algebraic system can be solved only with the iterative scheme proposed; moreover, due to the non linearity, it is not simply to analyze it theoretically. The Robin iteration procedure, being equally effective and accurate, does not present the above disavantages: matrix **A** does not change through the iterative procedure, no problems arise if $\phi_s^{(m)}=0$, the procedure is linear and, therefore, it has also been possible to study it theoretically.

7. NUMERICAL EXAMPLES AND PROCEDURE VALIDATION

In order to validate the Robin iteration procedure and to illustrate its practical application in concrete cases, in this section it is used for the numerical solution of four 2-D electromagnetic scattering problems and a 3-D acoustic one. The first example regards computation of the field scattered from a perfectly-conducting circular cylinder coated with a lossy dielectric, lighted by a plane wave. This example is also solved by means of the Bayliss, Gunzburger and Turkel ABC of first order (BGT_1); both the the numerical solutions are compared with the analytical one, which is known in this case. The second example concerns a perfectly-conducting square cylinder with smoothed corners, on which the surface current density is computed to compare it with other numerical results available in literature. The third example concerns two separate scatterers of different materials; this example has the aim of illustating the use of a multiple fictitious boundary. The fourth example concerns the scattering of a perfectly-conducting circular cylinder on a ground plane in order to show how such a plane can be dealt with by the procedure. The last example illustrates the 3-D procedure in the case of an acoustic plane wave which incides on a cube of perfectly soft material.

All these computations have been performed by means of the ELFIN code, a large finite element code developed by the authors for electromagnetic CAD research.[24,25] In particular a COCG solver with diagonal preconditioning was used.[28] The iterations performed by the solver are referred to as solver iterations, while the iterations relative to the iteration procedure are simply referred to as iterations or steps.

7.1. Perfectly-conducting circular cylinder coated with a lossy dielectric

Consider a plane (E- or H-polarized) wave $\phi_{inc} = e^{-jk_0 x}$ of wavelength λ which lights a perfectly-conducting circular cylinder, centered at the origin, of radius $R_C=2.25\lambda$, coated with a dielectric of thickness $R_d=\lambda/4$ (so the total radius of the scatterer is $R=2.5\lambda$). The dielectric medium is lossy having $\varepsilon_r=1.5\text{-}j0.8$ and $\mu_r=2\text{-}j$. A circular fictitious boundary Γ_F was selected and, according to (41), was placed at a distance $d=0.1\lambda$ from the dielectric surface. The air-dielectric interface was selected as the integration surface Γ_M. For symmetry reasons only half of the circular shell between the conductor and the fictitious boundary was discretized with a regular mesh of 1820 second-order triangular elements (130 subdivisions along φ, 7 along r, 2 of which outside the scatterer); curved elements were employed on the circular boundaries. This mesh is sufficiently fine to prevent the error due to the discretization from hiding the error due to the convergence tolerance δ_0, selected to 1% in this example. Choosing the optimal initial guess $\boldsymbol{\Psi}^{(0)}=\boldsymbol{\Psi}_{inc}$ for the Robin condition on the fictitious boundary, the procedure converges in 5 iterations. Table I reports the error indicator δ (defined by (A.14) in Appendix A) and the number of solver iterations for each iteration of the procedure.

The same E-polarized wave problem was also solved by means of BGT_1, with the fictitious boundary placed at a greater distance from the dielectric $d_1=0.5\lambda$. Ten layers of elements were used along the radial direction to discretize the air region (for a total of 3900 2nd-order triangles) so that the storage requirements were almost equivalent for the two methods. The solver needed 457 solver iterations to converge. The two numerical solutions were compared inside the dielectric with the analytical solution. The Robin iteration procedure shows a better performance: the Euclidean norm relative error on the solution obtained with the iterative method was 0.39% whereas the error on the BGT_1 solution was

10.5% and, in addition, the computing time required by the BGT_1 was almost twice that required by the Robin iteration procedure. Similar results were obtained in the H-polarized case.

7.2. Perfectly-conducting square cylinder with smoothed corners

The perfectly-conducting cylinder has a square cross section, whose sides are λ long, and smoothed corners, with smoothing radius equal to 0.040 λ (see Fig. 4). The fictitious boundary was homologously placed at d=0.060λ from the conductor surface; 4 layers of elements were interposed between them, whereas 96 subdivisions were made along the conductor surface (for a total of 1024 2nd-order elements). The convergence tolerance was set at 0.1%. As expected, in this second example the Robin iteration procedure showed a worse convergence behaviour than in the first one: for the E-polarized case 14 iterations were needed to gain the final result, with a total of 438 solver iterations. The absolute value of the surface current density (normalized with respect to the incident magnetic field strength) is reported in Fig. 5, where the abscissa represents the normalized distance measured along the MNP line, starting from the central point M of the left-hand side edge of the square. The same problem was also solved for a plane H-polarized wave and the result is shown in Fig. 6. In this latter calculation 8 iterations were needed with a total of 977 solver iterations.

Both these results are in good agreement with the ones obtained in [17] by means of the MoM method, which are reported as dotted lines in the same figures for the reader's convenience.

7.3. A multiple scatterer: a square lossy dielectric and a circular perfect conductor

This example shows the use of two separate parts of fictitious boundary enclosing two separate objects: a dielectric square cylinder whose edge is equal to 0.5333λ and a perfectly-conducting circular cylinder having a radius equal to the square edge. The dielectric is lossy with ε_r=1-0.2j and μ_r=2-0.5j. The incident wave is an E-polarized plane wave coming from the left. The fictitious boundary was selected as constituted of two closed curves homologous to the scattering objects. For this example the iterative procedure converged in 7 iterations. Fig.7 shows the contours of $\mathrm{Re}\{E_z\}$ and $\mathrm{Im}\{E_z\}$. In this example the splitting of the global algebraic system into two separate subsystems was exploited with a reduction in computing time of about 30%.

7.4. A scatterer on a ground plane

Consider a perfectly-conducting circular cylinder whose axis, say the z-axis, is parallel to a ground plane. The system is lighted by a plane electromagnetic wave $\phi'_{inc} = e^{-jk_0(x-y)/\sqrt{2}}$, E-polarized along the z-axis, which incides with an angle of π/4 with respect to the plane, as depicted in Fig. 8. The cylinder radius is R=λ/2 whereas the distance between its axis and the ground plane is H=λ. This example has the aim of showing the application of the Robin iteration procedure to the case of scattering in the presence of a ground plane. Two approaches are possible according to whether or not the ground plane constitutes a part of the boundary of the domain D in which the problem is to be solved. Of course in the first approach this part of boundary is not a fictitious boundary since a homogeneous Dirichlet conditions holds on it. The incident field ϕ_{inc} to be used in equation (8) is not that relative to the original wave ϕ'_{inc} only, but the wave $\phi''_{inc} = -e^{-jk_0(x+y)/\sqrt{2}}$, reflected by the ground plane,

has to be added so that $\phi_{inc} = \phi'_{inc} + \phi''_{inc} = 2e^{-jk_0 x/\sqrt{2}} \sin(k_0 y/\sqrt{2})$. Moreover the Green's function to be used in (7) must be modified into G(**r**,**r**') - G(**r**,**r**"), where **r**" is the symmetrical of **r**' with respect to the ground plane. In Fig. 9 the finite element mesh (972 triangles of 2nd-order) employed for the analysis is shown. In Fig. 10 the contours of Re{E_z}and Im{E_z } are plotted. The same problem was also solved by pursuing the second approach, that is, by enclosing the scatterer with a fictitious boundary which leaves out the ground plane. In Fig. 11 the contours of Re{E_z}and Im{E_z} are reported for a circular fictitious boundary. As can be seen the two solutions are in very good agreement.

7.5. A 3-D acoustic scatterer

Consider a perfectly-soft cube surrounded by air on which an acoustic plane wave incides normally to one cube side, travelling from the left in the x direction. The cube edge is equal to the wavelength λ. A cube fictitious boundary is selected homologous to the scatterer, having a side 1.4λ. Due to symmetry reasons only a quarter of the system was analyzed, imposing homogeneous Neumann boundary conditions on the xz and yz planes; a homogeneous Dirichlet condition holds on the scatterer surface. The resulting bounded domain was discretized with 2180 2nd-order tetrahedra, as shown in Fig. 12. Four iterations were needed to obtain convergence. The contours of Re{p} and Im{p}, where p is the air pressure, are depicted in Fig. 13.

8. CONCLUSIONS

In this paper a new method, named Robin iteration procedure, has been proposed for the FEM solution of 2-D and 3-D scalar scattering problems in open boundaries. The method has been first theoretically studied and then numerically validated by means of several examples of application. The method makes use of a Robin (mixed) condition on the fictitious boundary which resembles an absorbing boundary condition, but in the authors' opinion it does not belong to the class of ABC methods. In ABC methods a homogeneous condition is imposed on the fictitious boundary in order to simulate the unbounded medium, so that the main point of ABC lies in the choice of a good boundary operator. In the Robin iteration procedure a simple boundary operator can be used, allowing the nonhomogeneity of the condition. The Robin iteration procedure is an exact method which benefits from using some ABC features.

With the method presented here, scalar scattering problems can be solved efficiently at all frequencies for arbitrary systems without any interior resonance. The error in the solution is only due to the finite element discretization and to the convergence tolerance, which are selected by the user. The method is efficient in the sense that the region to be discretized is a small region around the scatterer surface and the number of iterations is low if the Robin operator and the initial guess for its value on the fictitious boundary are suitably selected. Another advantage of the iterative procedure relies on the simplicity of implementation in a pre-existing FE code for bounded problems.

ACKNOWLEDGEMENTS

This work has been partially supported by the MURST (the Italian Ministry for University and Scientific and Technological Research).

APPENDIX A: IMPLEMENTATION REMARKS

In this Appendix some implementation remarks are made illustrating the numerical computation of matrix **M** and the end-iteration test.

Numerical computation of matrix M

Assume that the closed curve (or surface) Γ_M be selected as constituted of a set *S* of element sides only (this choice is always possible). Calling S the generic side in this set and E the associated finite element external to Γ_M, one can develop the field ϕ inside E as:

$$\phi = \sum_{i=1}^{N_E} \phi_i \alpha_i \tag{A.1}$$

where α_i are the shape functions of the N_E nodes of the element E and ϕ_i are the nodal field values. Then by employing equation (7) to express the Robin condition in a nodal point $\mathbf{r} \in \Gamma_F$ one obtains:

$$\psi(\mathbf{r}) = \psi_{inc}(\mathbf{r}) - \sum_{S \in S} \sum_{i=1}^{N_E} \left(m_i' + m_i'' \right) \phi_i \tag{A.2}$$

where:

$$m_i' = \int_S \frac{\partial \alpha_i}{\partial n'} \left(\frac{\partial}{\partial n} + jk_0 \right) G(\mathbf{r}, \mathbf{r}') \, ds' \tag{A.3}$$

$$m_i'' = \int_S \alpha_i \left(\frac{\partial}{\partial n} + jk_0 \right) \frac{\partial}{\partial n'} G(\mathbf{r}, \mathbf{r}') \, ds' \tag{A.4}$$

Standard Gauss quadrature techniques can be used to evaluate the integrals in (A.3) and (A.4), since the integration domain $S \subset \Gamma_M$ does not contain the node **r**. Alternatively, if node **r** is

sufficiently far from E, a good approximation of the values of the Robin operator applied to the Green's function and its normal derivative are obtained by developing them inside E:

$$\left(\frac{\partial}{\partial n}+jk_0\right)G(\mathbf{r},\mathbf{r}')=\sum_{j=1}^{N_E}g_j\alpha_j \tag{A.5}$$

$$\left(\frac{\partial}{\partial n}+jk_0\right)\frac{\partial G(\mathbf{r},\mathbf{r}')}{\partial n'}=\sum_{j=1}^{N_E}f_j\alpha_j \tag{A.6}$$

Then:

$$m_i'=\sum_{j=1}^{N_E}g_j\int_S\frac{\partial\alpha_i}{\partial n'}\alpha_j\,ds' \tag{A.7}$$

$$m_i''=\sum_{j=1}^{N_E}f_j\int_S\alpha_i\alpha_j\,ds' \tag{A.8}$$

For triangular (or tetrahedral) elements with straight sides the integrals in (A.7) and (A,8) can be evaluated by resorting to Silvester's universal matrices.[2]

End-iteration test

In order to stop the iterative procedure one can utilize convergence tests commonly adopted for linear algebraic system solvers. Since convergence of vector $\boldsymbol{\Psi}$ implies convergence of vector $\boldsymbol{\Phi}$ and since the cardinality of the first is less than that of the second, it is convenient to adopt a convergence test in terms of the vector $\boldsymbol{\Psi}$ only, as for example:

$$\delta=100\frac{\left\|\boldsymbol{\Psi}_{res}^{(m)}\right\|_2}{\left\|\boldsymbol{\Psi}^{(m)}\right\|_2}<\delta_0 \tag{A.9}$$

where δ_0 is the end-iteration tolerance, selected by the user, and where $\boldsymbol{\Psi}_{\text{res}}^{(\text{m})}$ is the pseudo-residual vector at step m, given by:

$$\boldsymbol{\Psi}_{\text{res}}^{(\text{m})} = \boldsymbol{\Psi}^{(\text{m})} - \boldsymbol{\Psi}^{(\text{m}-1)} \tag{A.10}$$

Test (A.9), however, does not correctly measure the error $\boldsymbol{\Psi}_{\text{e}}^{(\text{m})}$ of the working solution with respect to the true solution $\boldsymbol{\Psi}_{\text{t}}$. In fact $\boldsymbol{\Psi}_{\text{e}}^{(\text{m})}$ and $\boldsymbol{\Psi}_{\text{res}}^{(\text{m})}$ are related as

$$\boldsymbol{\Psi}_{\text{e}}^{(\text{m})} = (\mathbf{P} - \mathbf{I})^{-1} \boldsymbol{\Psi}_{\text{res}}^{(\text{m})} \tag{A.11}$$

where matrix **P** is defined by (17) and **I** is the unit matrix of order N_F. Assuming $\|\mathbf{P}\|_2 < 1$, the error and pseudo-residual norms satisfy the inequality:[22]

$$\left\|\boldsymbol{\Psi}_{\text{e}}^{(\text{m})}\right\|_2 \le \left(1 - \|\mathbf{P}\|_2\right)^{-1} \left\|\boldsymbol{\Psi}_{\text{res}}^{(\text{m})}\right\|_2 \tag{A.12}$$

Of course the exact value of the norm of **P** is not known but it can be estimated while the iterations proceed by means of:

$$\text{p}^{(\text{m})} \cong \max_{\text{k}=1..\text{m}} \frac{\left\|\mathbf{P}\boldsymbol{\Psi}^{(\text{k})}\right\|_2}{\left\|\boldsymbol{\Psi}^{(\text{k}-1)}\right\|_2} \tag{A.13}$$

Then the iterative procedure is more significantly halted when:

$$\delta = \frac{100}{1 - p^{(m)}} \frac{\left\| \boldsymbol{\Psi}_{res}^{(m)} \right\|_2}{\left\| \boldsymbol{\Psi}^{(m)} \right\|_2} < \delta_0 \qquad \text{(A.14)}$$

APPENDIX B: A THEORETICAL STUDY OF THE PROCEDURE

In this appendix a theoretical study of the convergence of the Robin iteration procedure is made. From it useful insight will be obtained on the way in which the coefficient κ has to be chosen and how the method works. Although the study is carried out only with some restricting hypotheses, the method works under more general conditions.

Consider a system of scattering objects surrounded by free space, lighted by an incident wave. The total field satisfies the Helmholtz equation, whereas on the object surfaces $\#\#\#_C$ homogeneous Dirichlet or Neumann boundary conditions hold. Having selected a fictitious boundary Γ_F which encloses all the objects, a Robin boundary condition with $\kappa=jk_0$ is imposed on it.

As a first step in the study, two lemmas are proved which are similar to two theorems presented in [14]. The following norms are used throughout this appendix:

$$\|f\|_F = \left(\int_{\Gamma_F} |f|^2 d\Gamma\right)^{1/2} \qquad \|f\|_C = \left(\int_{\Gamma_C} |f|^2 d\Gamma\right)^{1/2} \tag{B.1}$$

LEMMA 1. Let ϕ be a function which satisfies the homogeneous Helmholtz equation (with k_0 real and positive) inside D, with homogeneous Dirichlet (or Neumann) conditions on the internal boundary $\#\#\#_C$ and a Robin condition on the external boundary $\#\#\#_F$:

$$\begin{aligned} &\nabla^2\phi + k_0^2\phi = 0 && \text{in D} \\ &\phi = 0 \quad (\partial\phi/\partial n = 0) && \text{on } \Gamma_C \\ &\frac{\partial\phi}{\partial n} + jk_0\phi = \psi && \text{on } \Gamma_F \end{aligned} \tag{B.2}$$

Then the following bounds hold:

$$\|\phi\|_F \le \frac{\|\psi\|_F}{k_0} \tag{B.3}$$

$$\left\|\frac{\partial \phi}{\partial n}\right\|_F \le 2\|\psi\|_F \tag{B.4}$$

Proof. Multiply the Helmholtz equation by the complex conjugate ϕ^* of the field, and integrate over D. Applying the first Green theorem to the first term and taking into account the boundary condition on ###C, we obtain:

$$-\int_D |\nabla\phi|^2 dD + k_0^2 \int_D |\phi|^2 dD = -\int_{\Gamma_F} \phi^* \frac{\partial \phi}{\partial n} d\Gamma = -\int_{\Gamma_F} \phi^* (\psi - jk_0\phi) d\Gamma \tag{B.5}$$

The left-hand side term is purely real, so the imaginary part of the right-hand one must vanish; thus

$$k_0 \int_{\Gamma_F} |\phi|^2 d\Gamma = \mathrm{Im}\left\{\int_{\Gamma_F} \phi^* \psi \, d\Gamma\right\} \le \|\phi\|_F \|\psi\|_F \tag{B.6}$$

from which (B.3) follows immediately. Inequality (B.4) is derived from:

$$\left\|\frac{\partial \phi}{\partial n}\right\|_F = \|\psi - jk_0\phi\|_F \le \|\psi\|_F + k_0\|\phi\|_F \le 2\|\psi\|_F \tag{B.7}$$

LEMMA 2 Consider the same boundary-value problem of lemma 1. Assume that the external boundary ###$_F$ be a circle (or a sphere) of radius R_F centered at the origin. Then there exists a constant C, independent of R_F, such that:

$$\left\| \frac{\partial \phi}{\partial n} \right\|_C \le C \left(\|\phi\|_F + \left\| \frac{\partial \phi}{\partial n} \right\|_F \right) \qquad \text{(Dirichlet)} \qquad \text{(B.8)}$$

$$\|\phi\|_C \le C \left(\|\phi\|_F + \left\| \frac{\partial \phi}{\partial n} \right\|_F \right) \qquad \text{(Neumann)} \qquad \text{(B.9)}$$

Proof. Only the Neumann case will be proved, the demonstration of the Dirichlet one being quite similar. Applying to ϕ the Green's theorem in the bounded domain D, at a point $\mathbf{r} \in$ ###$_C$ we have:

$$\begin{aligned} \frac{1}{2}\phi(\mathbf{r}) &= \int_{\Gamma_F} \left[U(\mathbf{r},\mathbf{r}') \frac{\partial \phi(\mathbf{r}')}{\partial n'} - \phi(\mathbf{r}') \frac{\partial U(\mathbf{r},\mathbf{r}')}{\partial n'} \right] d\Gamma - \int_{\Gamma_C} \phi(\mathbf{r}') \frac{\partial U(\mathbf{r},\mathbf{r}')}{\partial n'} d\Gamma \\ &= \zeta(\mathbf{r}) - \int_{\Gamma_C} \phi(\mathbf{r}') \frac{\partial U(\mathbf{r},\mathbf{r}')}{\partial n'} d\Gamma \end{aligned} \qquad \text{(B.10)}$$

where U(**r**,**r'**) denotes the modified Green's function of Ursell.[29] The first term on the right-hand side satisfies the bound

$$\|\zeta\|_C \le C_1 \left(\|\phi\|_F + \left\| \frac{\partial \phi}{\partial n} \right\|_F \right) \qquad \text{(B.11)}$$

with C_1 independent of the radius of ###$_F$. Equation (B.10) can be interpreted as a Fredholm integral equation of the second kind for ϕ on ###$_C$. By virtue of the properties of the modified Green's function of Ursell (used in place of the free-space Green's function) the corresponding homogeneous integral equation only has the trivial solution $\phi=0$.[29] Then the continuous linear operator $\Theta(\phi)=\zeta$ is invertible and, according to the Banach theorem, the inverse operator Θ^{-1} is a continuous linear operator. Then there exists a constant C_2 such that:

$$\|\phi\|_C = \left\|\Theta^{-1}(\zeta)\right\|_C \le C_2\|\zeta\|_C \tag{B.12}$$

Taking into account (B.11), inequality (B.9) follows immediately with $C=C_1C_2$.

Making use of these two lemmas the theorem stated in Sect. 3 can be proved. This theorem is concerned with the error functions at step m in the Robin iteration procedure, that is to say the difference betweeen the field and the Robin boundary condition at step m and those relative to the solution of the unbounded problem:

$$\psi_e^{(m)} = \psi^{(m)} - \psi_t \tag{B.13}$$

$$\phi_e^{(m)} = \phi^{(m)} - \phi_t \tag{B.14}$$

THEOREM For a system of scattering objects on whose surfaces homogeneous Dirichlet (or Neumann) conditions hold, enclosed by a circular (or spherical) fictitious boundary of radius R_F on which a Robin condition (with $\kappa=jk_0$) is imposed, the sequence of the Robin condition errors is such that:

$$\left\|\psi_e^{(m)}\right\|_F \le \bar{\rho}^m \left\|\psi_e^{(0)}\right\|_F \qquad \forall\ m = 1,2,\ldots\infty \tag{B.15}$$

where $\bar{\rho}$ is a suitable real constant, depending on geometry only, which vanishes asymptotically as $O(R_F^{-1})$ as $R_F \to \infty$.

Proof. Let us first consider the case in which a homogeneous Dirichlet boundary condition holds on ###C, which is the simpler one. As a first step in the proof, note that the Robin iteration procedure is linear, so the field error function $\phi_e^{(m)}$ solves the following boundary-value problem:

$$\begin{aligned} &\nabla^2\phi_e^{(m)} + k_0^2\phi_e^{(m)} = 0 && \text{in } D \\ &\phi_e^{(m)} = 0 && \text{on } \Gamma_C \\ &\frac{\partial\phi_e^{(m)}}{\partial n} + jk_0\phi_e^{(m)} = \psi_e^{(m)} && \text{on } \Gamma_F \end{aligned} \tag{B.16}$$

Using the bounds derived in lemmas 1 and 2, we obtain

$$\left\|\frac{\partial\phi_e^{(m)}}{\partial n}\right\|_C \le T\left\|\psi_e^{(m)}\right\|_F \tag{B.17}$$

where T is a constant independent of the radius R_F of ###F.

Now, using formula (7) with ###M ≡ ###C and taking into account the homogeneous Dirichlet condition on Γ_C, the error on the new Robin condition on Γ_F is obtained:

$$\psi_e^{(m+1)}(\mathbf{r}) = -\int_{\Gamma_C} \frac{\partial \phi_e^{(m)}(\mathbf{r}')}{\partial n'} \left(\frac{\partial}{\partial n} + jk_0 \right) G(\mathbf{r}, \mathbf{r}') \, d\Gamma' \qquad \text{(B.18)}$$

and applying the Schwartz inequality:

$$\left| \psi_e^{(m+1)}(\mathbf{r}) \right| \leq \left\| \frac{\partial \phi_e^{(m)}(\mathbf{r}')}{\partial n'} \right\|_C \left\| \left(\frac{\partial}{\partial n} + jk_0 \right) G(\mathbf{r}, \mathbf{r}') \right\|_C \qquad \text{(B.19)}$$

Squaring this inequality, integrating over ###$_C$ and taking into account (B.17), we obtain:

$$\left\| \psi_e^{(m+1)} \right\|_F \leq \bar{\rho} \left\| \psi_e^{(m)} \right\|_F \qquad \text{(B.20)}$$

where:

$$\bar{\rho} = \sqrt{T \int_{\Gamma_C} \int_{\Gamma_F} \left| \left(\frac{\partial}{\partial n} + jk_0 \right) G(\mathbf{r}, \mathbf{r}') \right|^2 d\Gamma \, d\Gamma'} \qquad \text{(B.21)}$$

Owing to the fact that ###$_C$ is a circumference centered at the origin it is easy to see that

$$\left(\frac{\partial}{\partial n} + jk_0 \right) G(\mathbf{r}, \mathbf{r}') = O\left(R_F^{-3/2} \right) \quad \text{as} \quad R_F \to \infty \qquad \text{(B.22)}$$

The measure of ###$_F$ raises as R_F does so the integral on it goes to zero as $O(R_F^{-2})$. Finally, taking into account the square root, we have:

$$\overline{\rho} = O\left(R_F^{-1}\right) \quad \text{as} \quad R_F \to \infty \tag{B.23}$$

The same result (B.23) applies in 3-D, since in this case the behaviour of (B.22) is $O\left(R_F^{-2}\right)$ and the measure of $\#\#\#_F$ raises as R_F^2 does.

Then the circular or spherical fictitious boundary can be placed sufficiently far from the scattering objects in such a way that $\overline{\rho}<1$ and the iterative procedure converges to the exact solution.

For the case of Neumann boundary conditions on $\#\#\#_C$ the theorem can be proved as follows. From lemma 2 we have:

$$\left\|\phi_e^{(m)}\right\|_C \le S\left\|\psi_e^{(m)}\right\|_F \tag{B.24}$$

where S, like T, is a constant independent of proportional deformations of $\#\#\#_F$. Applying (7) with $\#\#\#_M \equiv \#\#\#_C$ and taking into account the homogeneous Neumann boundary condition on Γ_C, the error on the new Robin condition on Γ_F is obtained:

$$\psi_e^{(m+1)}(\mathbf{r}) = -\int_{\Gamma_C} \phi_e^{(m)}(\mathbf{r}')\left(\frac{\partial}{\partial n} + jk_0\right)\frac{\partial G(\mathbf{r},\mathbf{r}')}{\partial n}\,d\Gamma' \tag{B.25}$$

Using the Schwartz inequality and manipulating the resulting expression as before, we again obtain (B.20) in which:

$$\overline{\rho} = \sqrt{S \int_{\Gamma_C} \int_{\Gamma_F} \left| \left(\frac{\partial}{\partial n} + jk_0 \right) \frac{\partial G(\mathbf{r}, \mathbf{r}')}{\partial n'} \right|^2 d\Gamma \, d\Gamma'} \tag{B.26}$$

It can easily be seen that this contraction coefficient has the same behaviour as (B.21). This completes the proof.

REFERENCES

1. O. C. Zienkiewicz and R. I. Taylor, *The Finite Element Method,* McGraw-Hill, Maidenhead, 1991.

2. P. P. Silvester and R. L. Ferrari, *Finite Elements for Electrical Engineers*, Cambridge University Press, Cambridge, 1990.

3. P. Bettess, 'Finite element modelling of exterior electromagnetic problems,' *IEEE Transactions on Magnetics*, vol. 24, no. 1, pp. 238-243, January 1988.

4. C.R.I. Emson, 'Methods for the solution of open boundary electromagnetic-field problems,' *IEE Proceedings,* vol. 135, no. 1, pp. 151-158, March 1988

5. C. A. Brebbia, *The Boundary Element Method for Engineers*, Pentech Press, London, 1978.

6. C.W. Trowbridge, 'Integral equations in electromagnetics,' *International Journal of Numerical Modelling: Electronic Networks, Devices and Fields*, vol. 9, 1996, pp. 3-17.

7. R. F. Harrington, *Field Computation by Moment Methods*, MacMillan, New York, 1968.

8. J. Moore and R. Pizer, *Moment Methods in Electromagnetics*, Research Studies Press, Letchworth, 1984.

9. B. H. McDonald and A. Wexler, 'Finite-element solution of unbounded field problems,' *IEEE Transactions on Microwave Theory and Techniques*, vol. 20, pp.841-847, December 1972.

10. J-M. Jin and V. V. Liepa, 'Application of hybrid finite element method to electromagnetic scattering from coated cylinders,' *IEEE Tranactions on Antennas and Propagation*, vol. 36, no.1, pp. 50-54, Jan. 1988.

11. P. Bettess, 'Infinite elements,' *International Journal for Numerical Methods in Engineering*, vol.11, pp. 53-64, 1977.

12. O. C. Zienkiewicz, K. Bando, P. Bettess, C. Emson and T. C. Chiam, 'Mapped infinite elements for exterior wave problems,' *International Journal for Numerical Methods in Engineering*, vol. 21, pp. 1229-1251, 1985.

13. B. Engquist and A. Majda, 'Radiation boundary conditions for the numerical simulation of waves,*' Math. Comp*., vol. 31, pp. 629-651, 1977.

14. A. Bayliss, M. Gunzburger and E. Turkel, 'Boundary conditions for the numerical solution of elliptic equations in exterior regions*,' SIAM Journal Applied Mathematics*, vol. 42, no. 2, pp. 430-451, 1982

15. O.M. Ramahi, A. Khebir and R. Mittra, 'Numerically derived absorbing boundary condition for the solution of open region scattering problems,' *IEEE Transactions on Antennas and Propagation*, vol. 39, no.3, pp. 350-353, March 1991.

16. Y. Li and Z. Cendes, 'High-accuracy absorbing boundary conditions,' *IEEE Tranactions on Magnetics*, vol. 31, no.3, pp. 1524-1529, May 1995.

17. K. K. Mei, R. Pous, Z. Chen, Y-W Liu and M. D. Prouty, 'Measured equation of invariance: a new concept in field computations,' *IEEE Transactions on Antennas and Propagations*, vol. 42, no.3, pp. 320-328, March 1994.

18 G. Aiello, S. Alfonzetti, S. Coco, 'Charge iteration: a procedure for the finite element computation of unbounded electrical fields, *Inernational Journal for Numerical Methods in Engineering*, vol. 37, no. 24, pp. 4147-4166, December 1994.

19 G. Aiello, S. Alfonzetti, S. Coco, and N. Salerno, 'Current iteration for unbounded skin-effect problems,' *COMPEL*, vol. 13, suppl. A, pp. 299-304, May 1994.

20 G. Aiello, S. Alfonzetti, S. Coco, and N. Salerno, 'Finite element iterative solution of skin effect problems in open boundaries,' *International Journal of Numerical Modelling: Electronic Networks, Devices and Fields*, vol. 9, pp. 125-144, 1996.

21. J. Van Bladel, *Electromagnetic Fields*, Hemisphere Publishing Corporation, New York, 1985.

22. L. A. Hageman and D. M. Young, *Applied Iterative Methods*, Academic Press, San Diego, 1981.

23. K. Fujiwara, T. Nakata and H. Fusayasu, 'Acceleration of convergence characteristic of the ICCG method,' *IEEE Tranactions on Magnetics*, vol. 29, no. 2, pp. 1958-61, March 1993

24. S. Alfonzetti and S. Coco, 'ELFIN: an N-dimensional finite element code for the computation of electromagnetic fields,' *IEEE Transactions on Magnetics*, vol. 24, no.1, 1988, pp. 362-365.

25. G. Aiello, S. Alfonzetti, S. Coco and N. Salerno, 'An FEM code for electrical engineering research: ELFIN,' ELECTROSOFT'96, San Miniato (I), 28-30 May 1966, pp. 357-366.

26. K. K. Mei, 'Unimoment method of solving antenna and scattering problems,' *IEEE Transactions on Antennas and Propagations*, vol. 22, no.6, pp. 760-766, 1974.

27. P. Steyn and D.B. Davidson, 'A technique for avoiding the EFIE "interior resonance" problem applied to an MM solution of electromagnetic radiation from bodies of revolution,' *ACES Journal*, vol. 10, no. 3, pp. 116-128, 1995.

28. H. A. van der Vorst and J. B. M. Melissen, ‘A Petrov-Galerkin type method for solving *Ax=b* when *A* is symmetric complex,’ *IEEE Transactions on Magnetics*, Vol. 26, No. 2, pp. 706-708, March 1990.

29. F. Ursell, ‘On the exterior problems of acoustic,’ *Proceedings of the Cambridge Philosophycal Society*, vol. 74, pp.117-125, 1972.

TABLE I

Error indicator and solver iterations in the procedure for example 7.1 (E-polarized case).

Iteration	Error indicator	Solver iterations
0	-	69
1	23.5%	50
2	9.21%	47
3	3.67%	27
4	1.43%	26
5	0.25%	-

FIGURE LEGENDS

Fig. 1 - Multiple scattering objects enclosed by a fictitious boundary.

Fig. 2 - Plot of the distance d_n versus R_F in the E-polarized case.

Fig. 3 - Plot of the distance d_n versus R_F in the H-polarized case.

Fig. 4 - Square cylinder with smoothed corners and associated fictitious boundary.

Fig. 5 - Behaviour of the current density magnitude |J| on the square scatterer surface (E-polarized case)

Fig. 6 - Behaviour of the current density magnitude |J| on the square scatterer surface (H-polarized case)

Fig. 7 a,b - Contours of the real and imaginary parts of E_z for the multiple scatterer

Fig. 8 - A circular cylinder on a ground plane.

Fig. 9 - Finite element mesh for the circular cylinder on a ground plane

Fig. 10 a,b - Contours of the real and imaginary parts of E_z for the scatterer on a ground plane

Fig. 11 a,b - Contours of the real and imaginary parts of E_z for the scatterer on a ground plane (which is outside the fictitious boundary).

Fig. 12 - Finite element mesh for the acoustic cube scatterer

Fig. 13 a,b - Contours of the real and imaginary part of the air pressure around the cube scatterer.

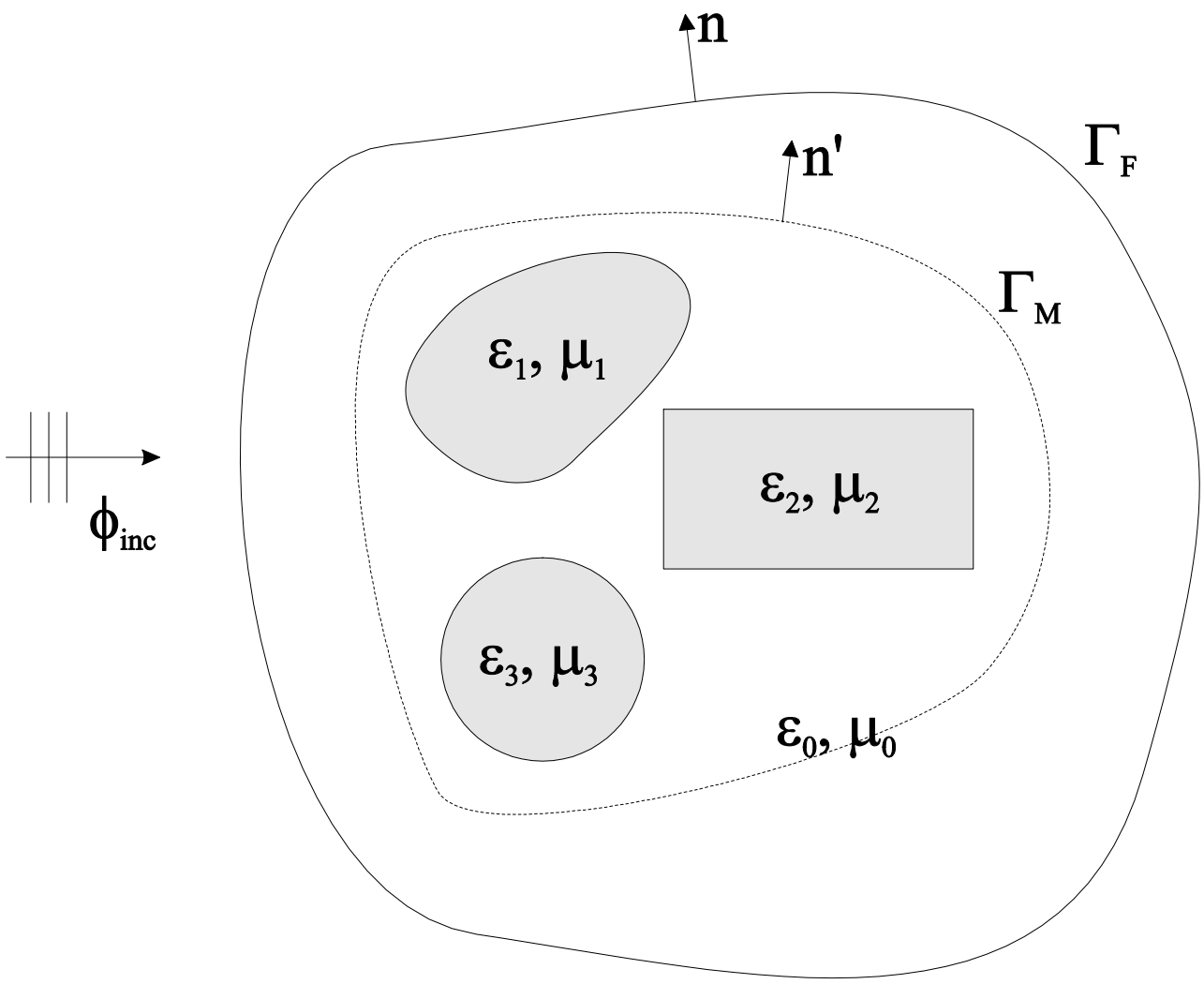
n
n'
Γ_F
Γ_M
ε_1, μ_1
ε_2, μ_2
ε_3, μ_3
ε_0, μ_0
ϕ_{inc}

Fig. 1

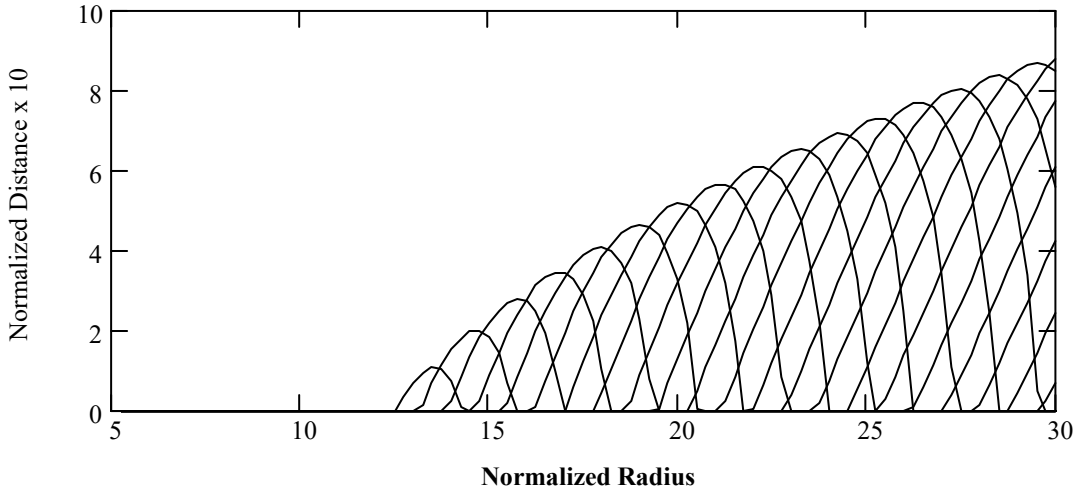
Normalized Distance x 10
10
8
6
4
2
0
5
10
15
20
25
30
Normalized Radius

Fig. 2

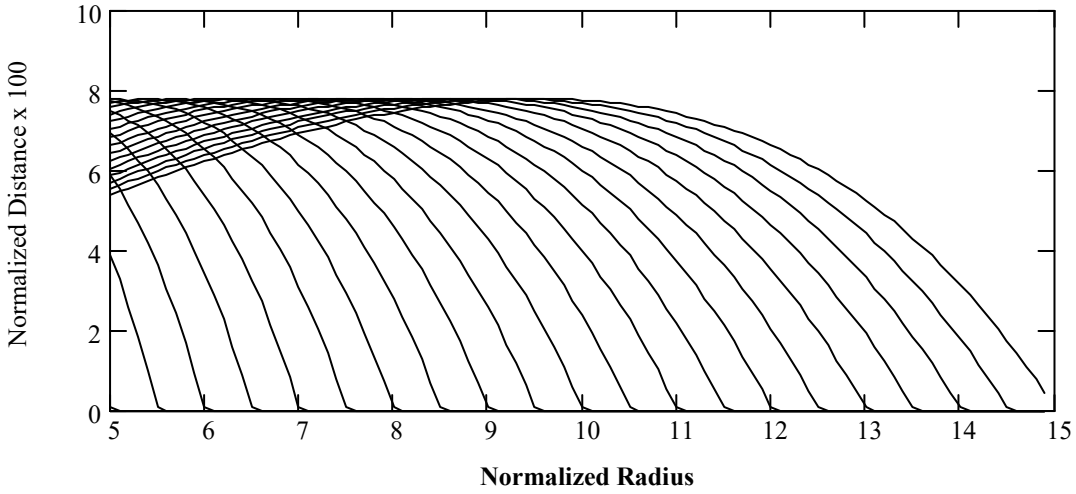
Normalized Distance x 100
10
8
6
4
2
0
5
6
7
8
9
10
11
12
13
14
15
Normalized Radius

Fig. 3

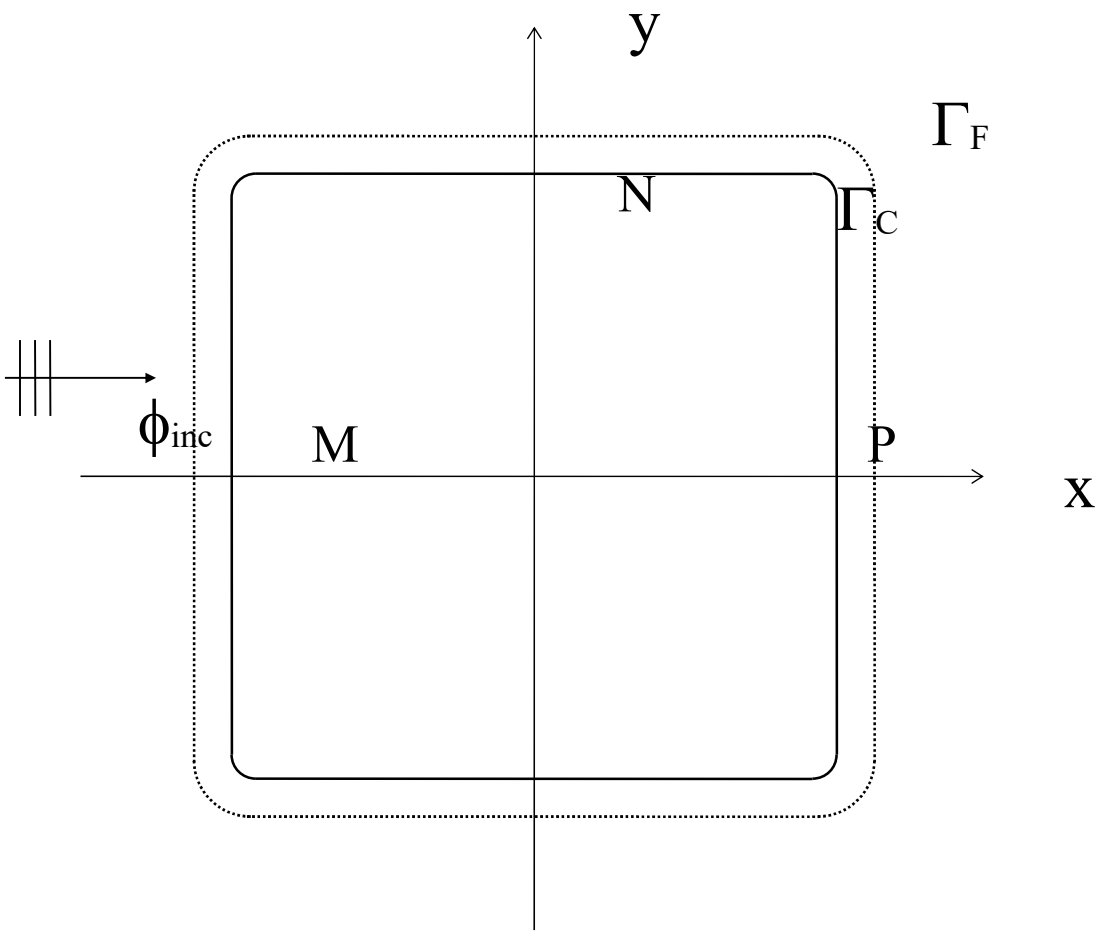

Fig. 4

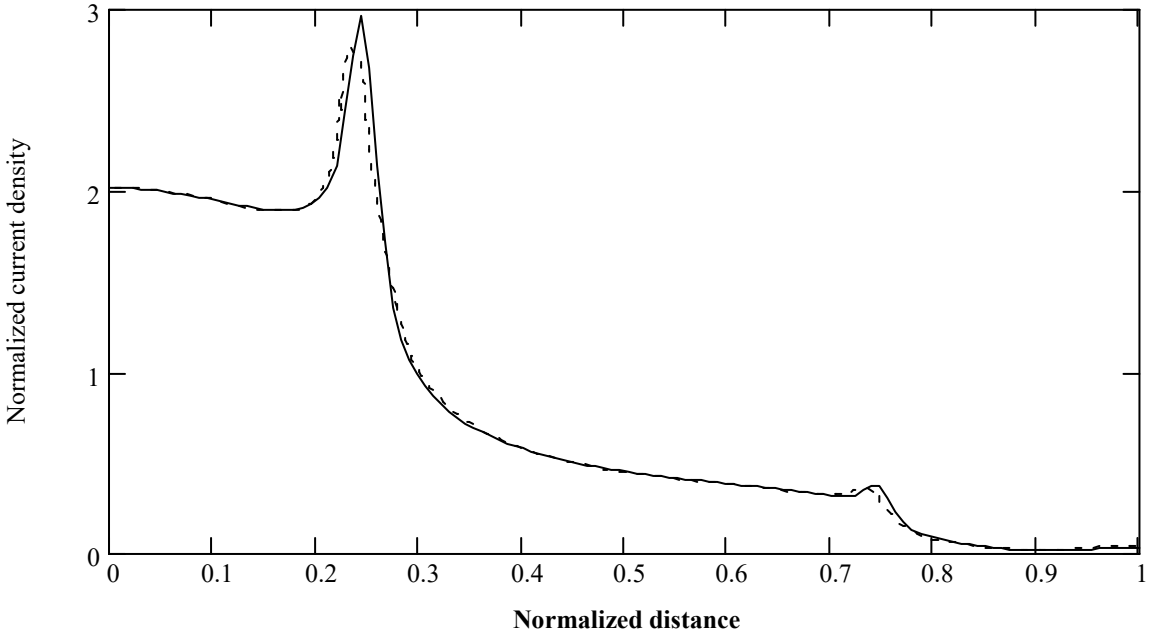
Normalized current density
3
2
1
0
0
0.1
0.2
0.3
0.4
0.5
0.6
0.7
0.8
0.9
1
Normalized distance

Fig. 5

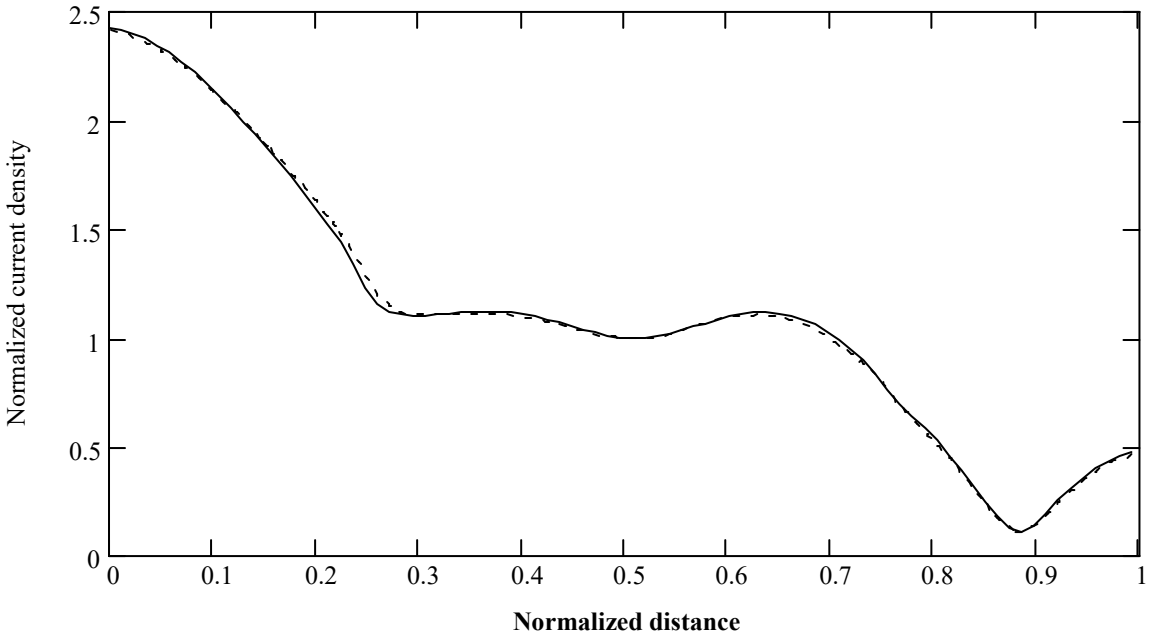
Normalized current density
2.5
2
1.5
1
0.5
0
0
0.1
0.2
0.3
0.4
0.5
0.6
0.7
0.8
0.9
1
Normalized distance

Fig. 6

Fig. 7a

Fig. 7b

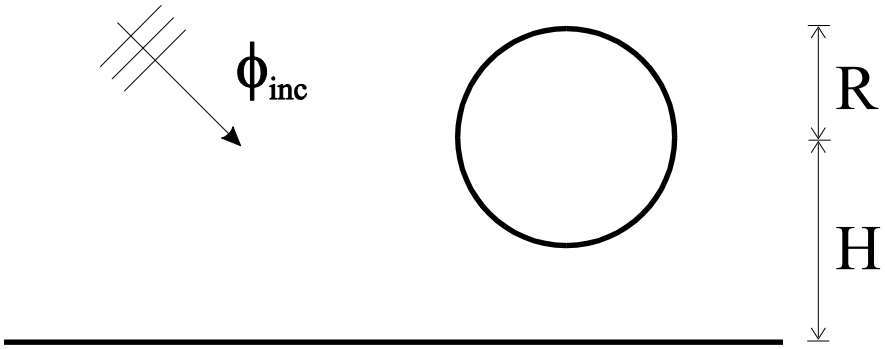

Fig. 8

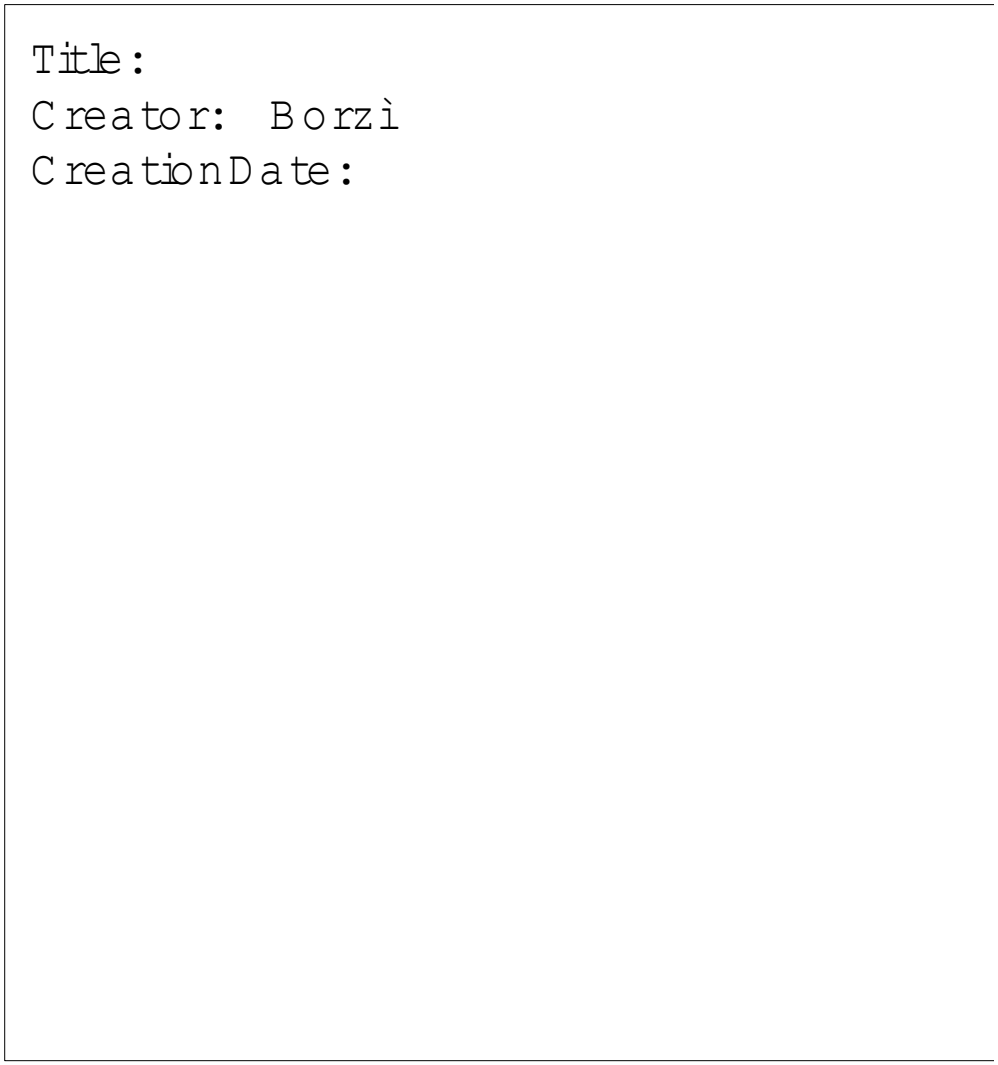

Fig. 9

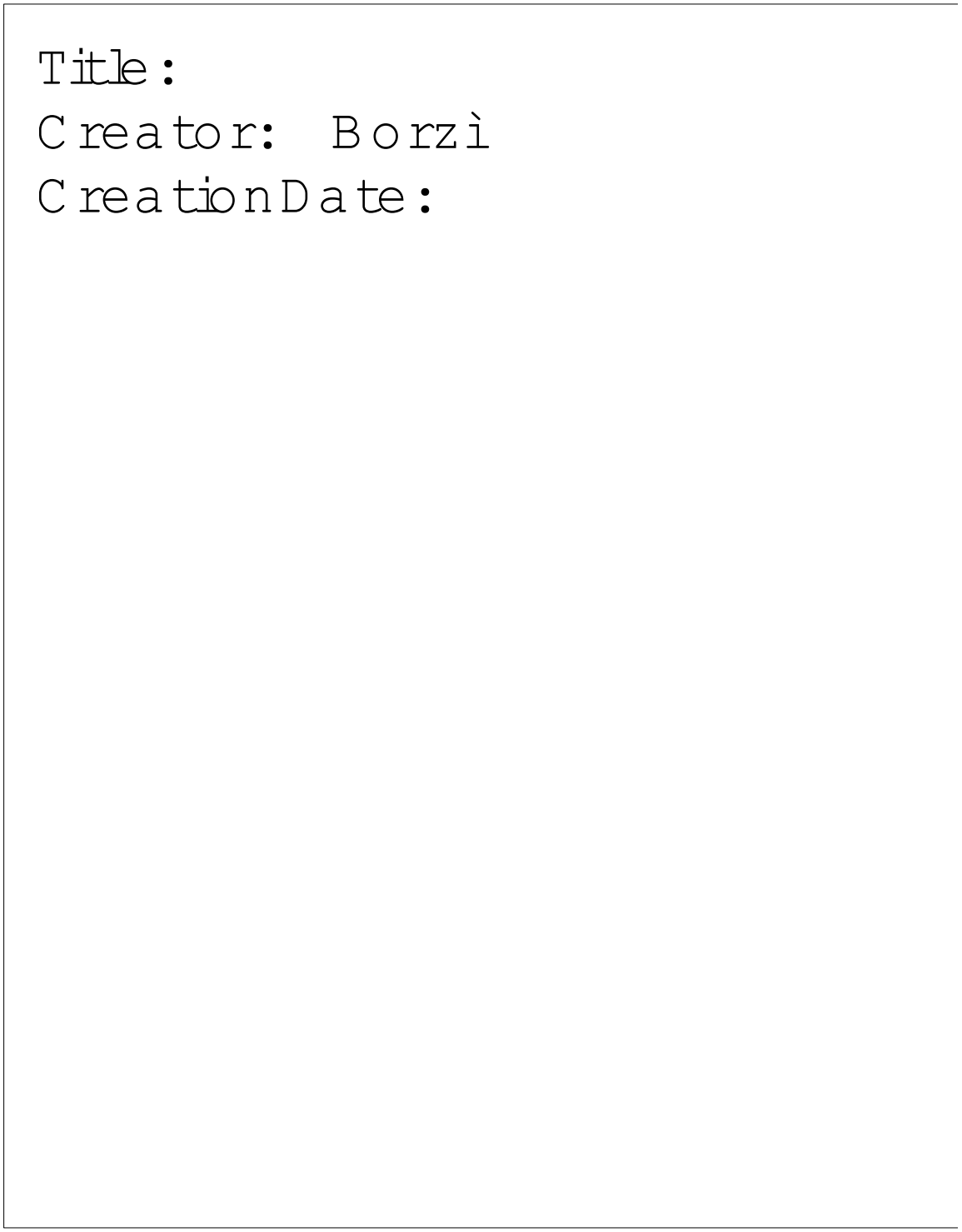

$\mathrm{Re}\{E_z\}$

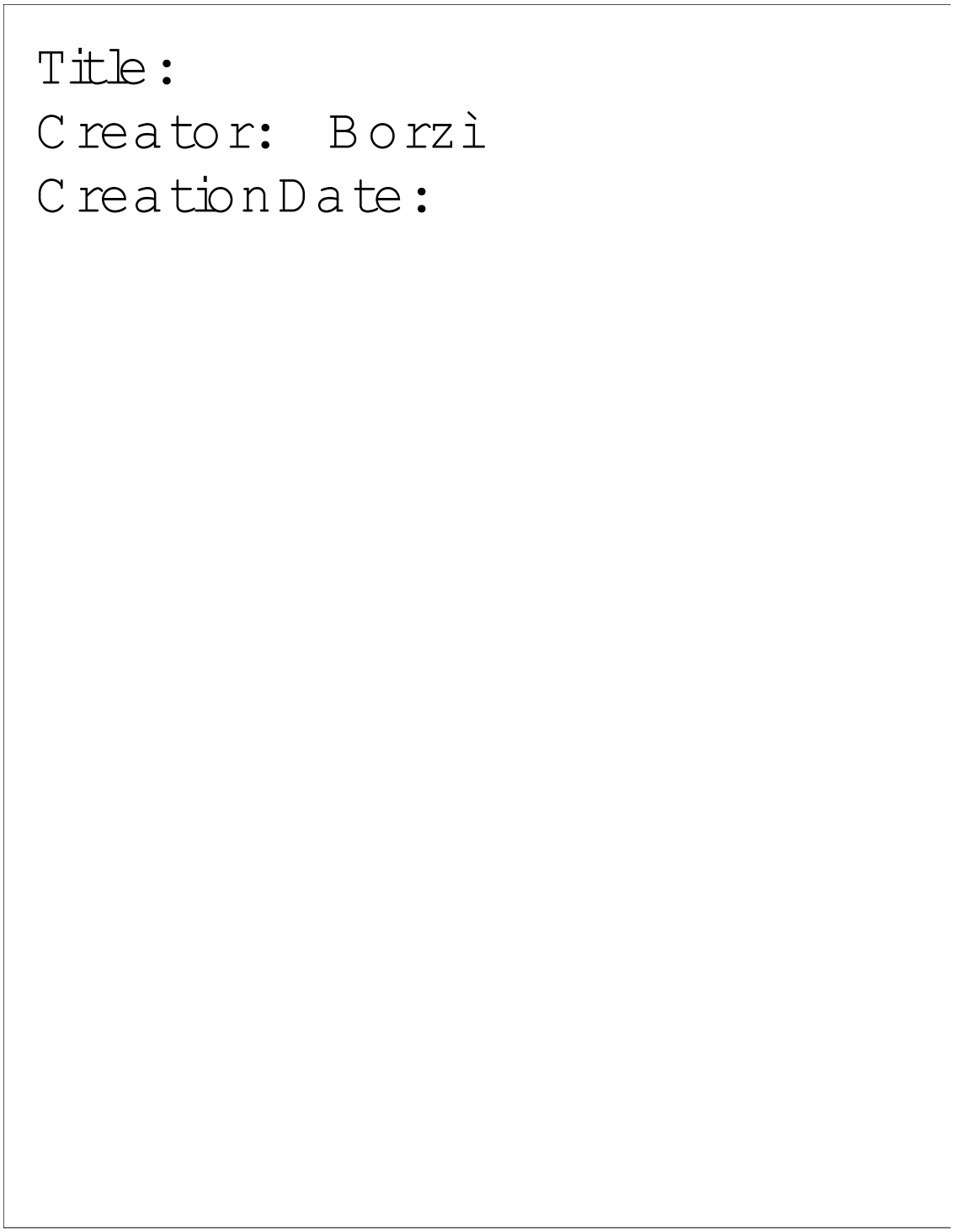

$\mathrm{Im}\{E_z\}$

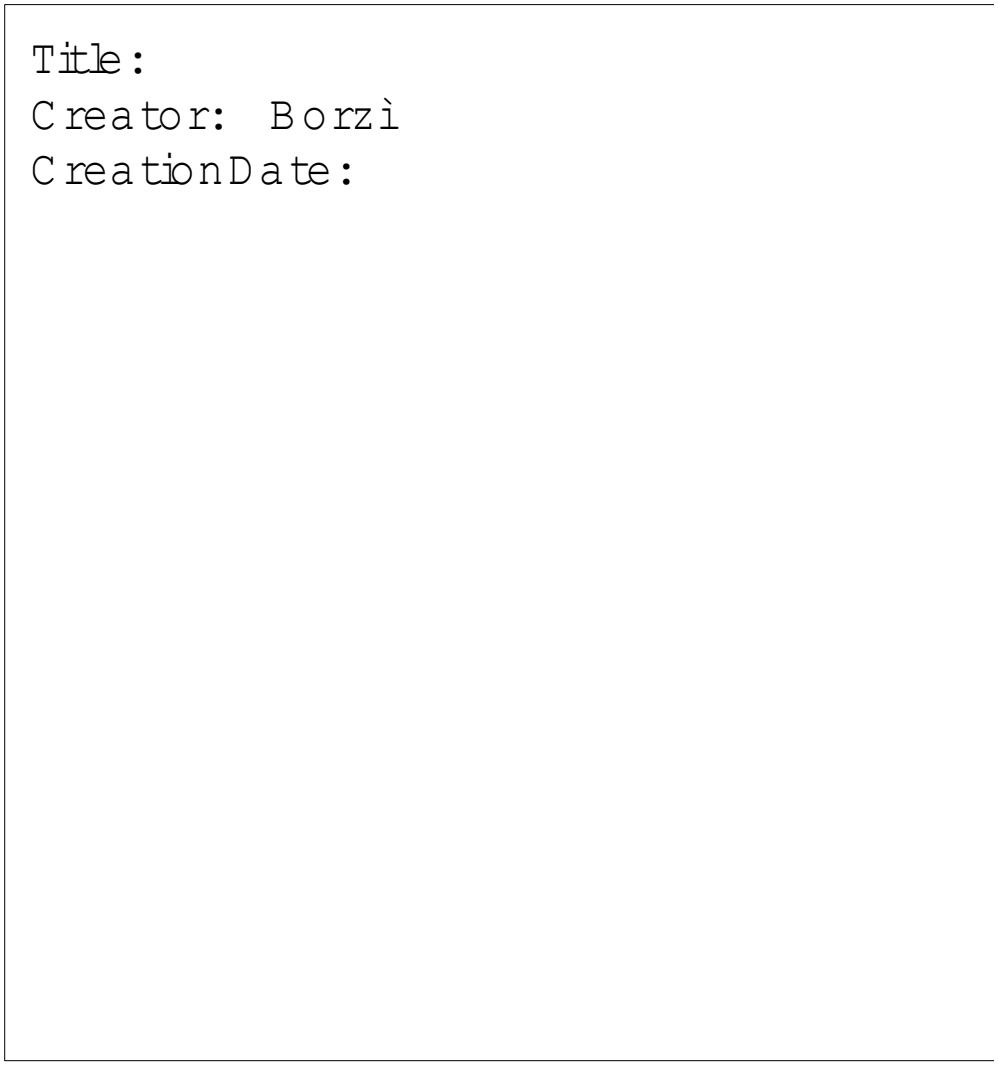

Fig. 11a

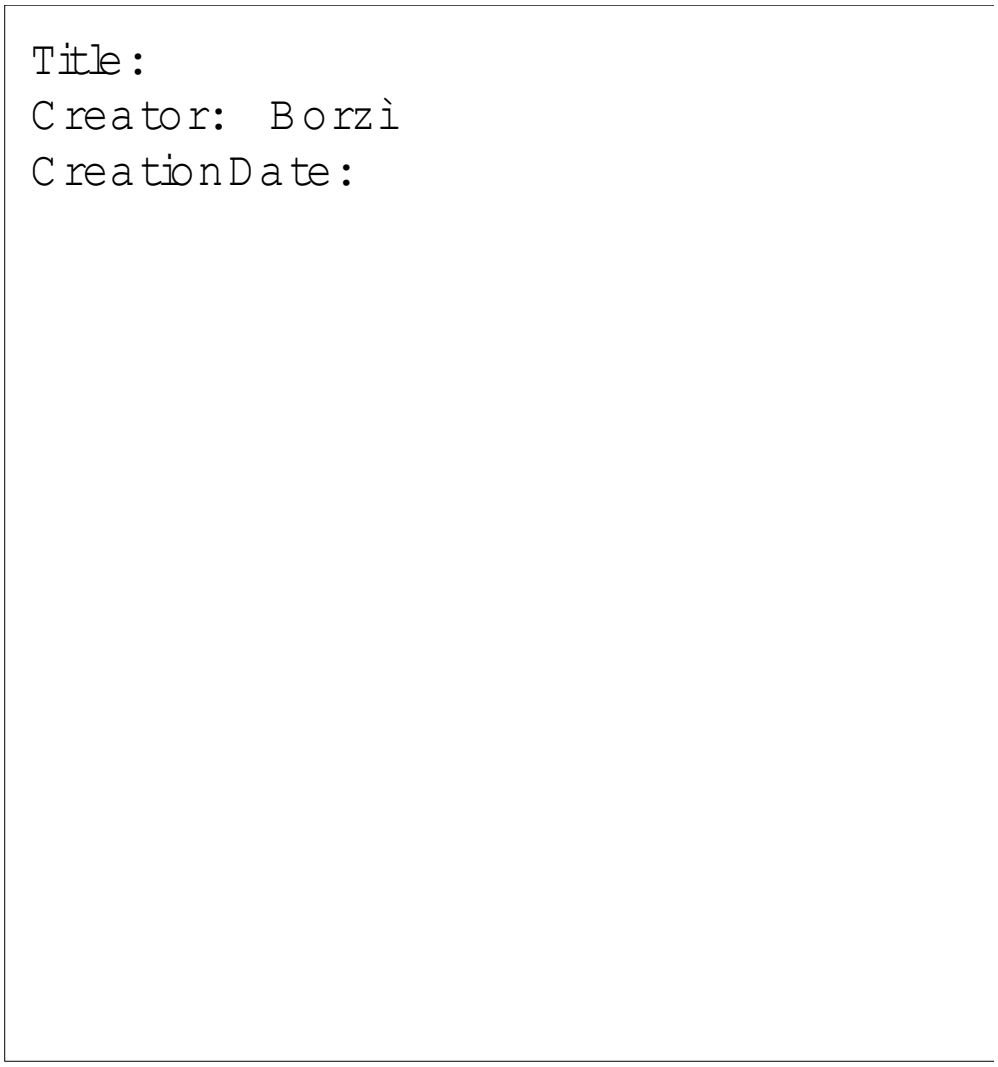

Fig. 11b

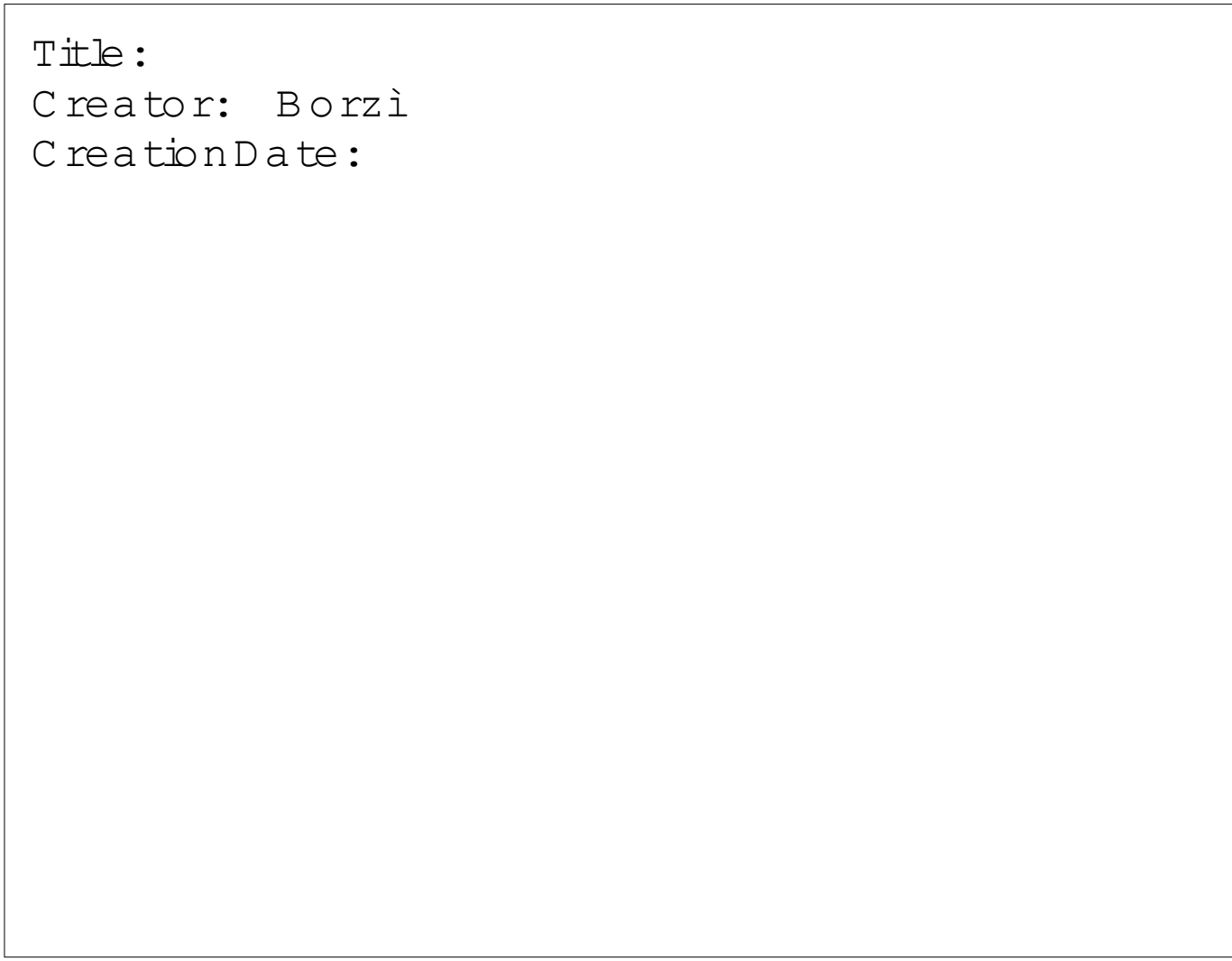

Fig. 12

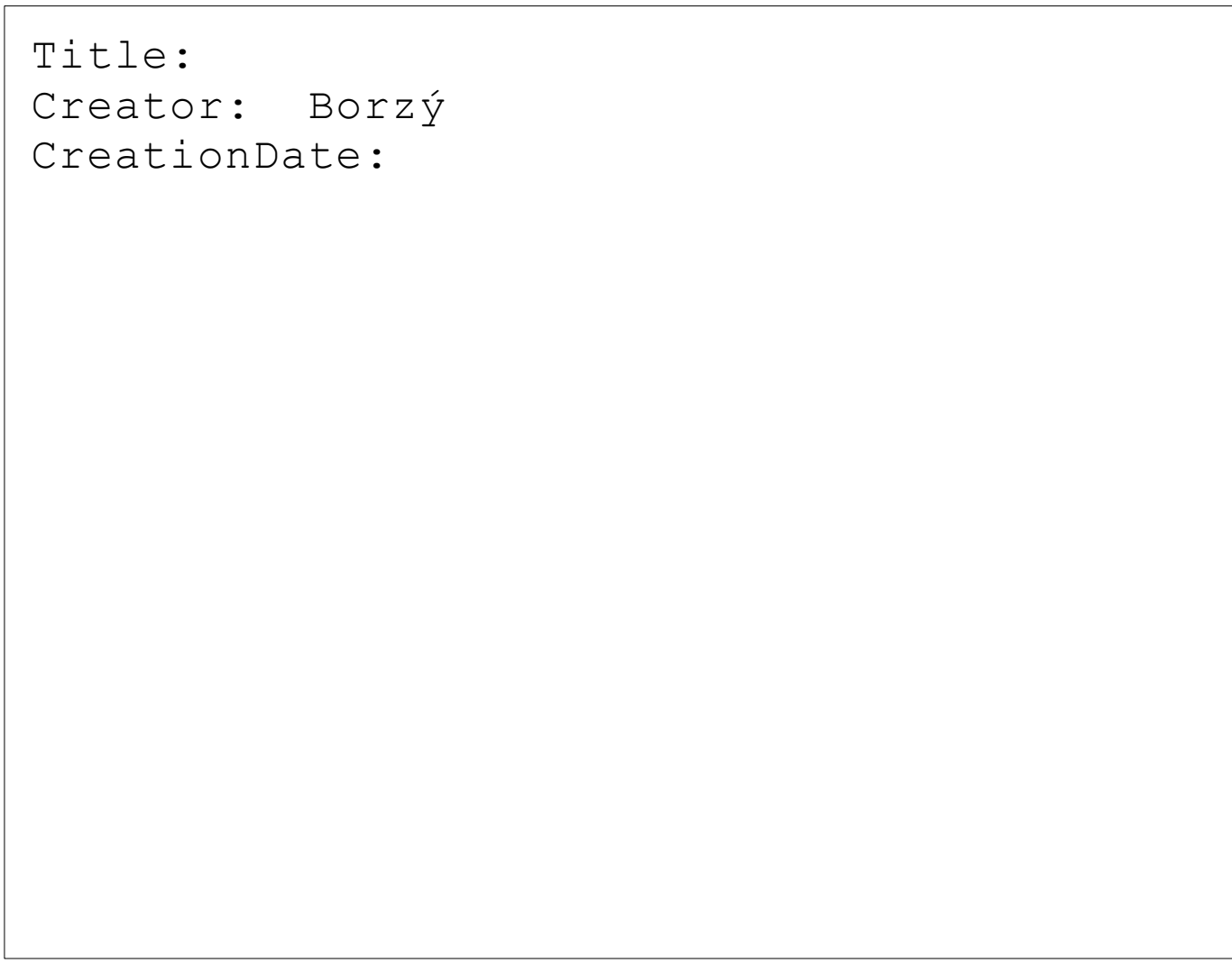

Fig. 13a

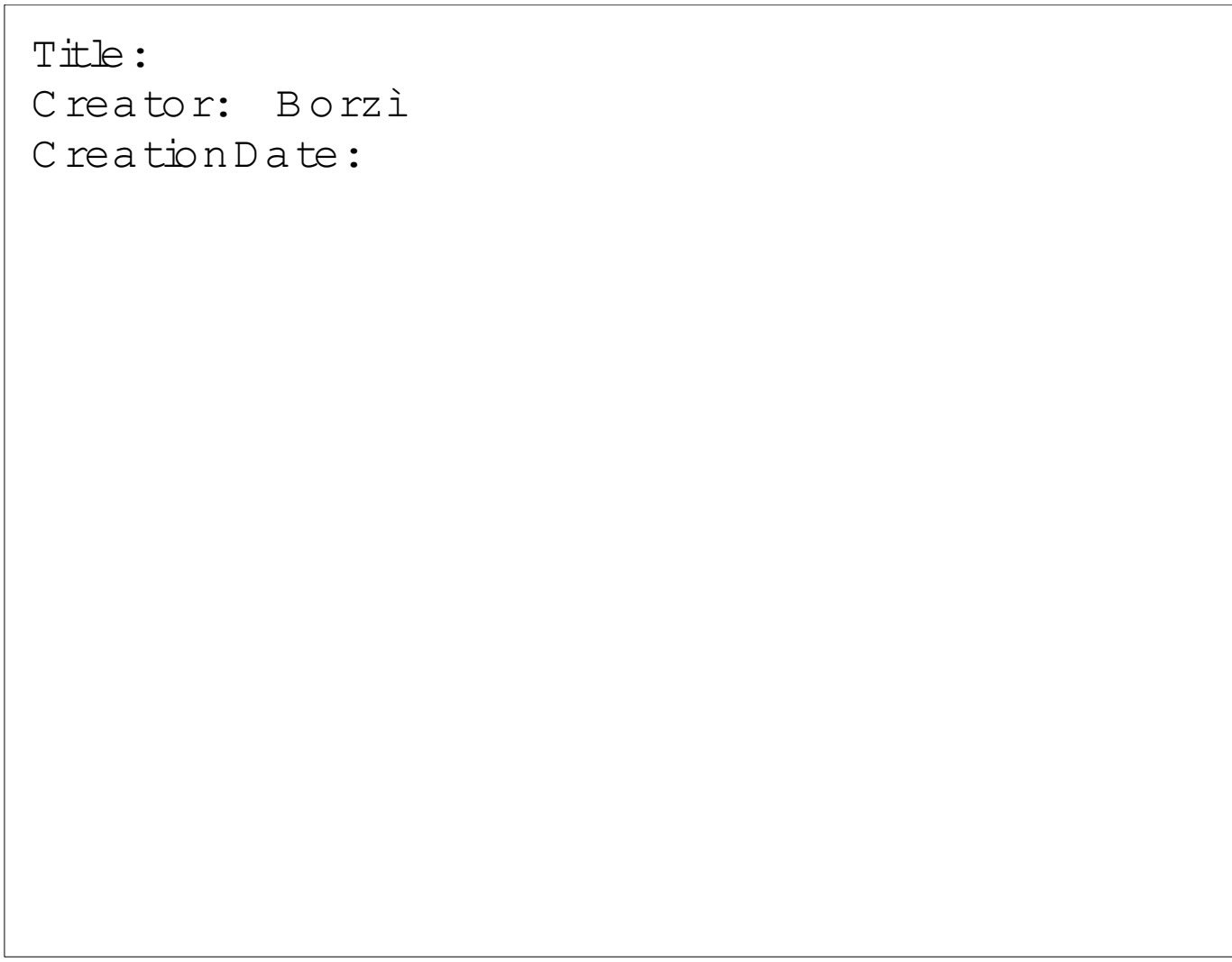

Fig. 13b